Cell Biology
Stem Cells and Regenerative Medicine

Differential regulation by CD47 and thrombospondin-1 of extramedullary erythropoiesis in mouse spleen

Reviewed Preprint
v2 • May 29, 2024
Revised by authors

Reviewed Preprint
v1 • November 22, 2023

Rajdeep Banerjee, Thomas J. Meyer, Margaret C. Cam, Sukhbir Kaur, David D. Roberts

Laboratory of Pathology, Center for Cancer Research, National Cancer Institute, National Institutes of Health, Bethesda, MD, USA • CCR Collaborative Bioinformatics Resource, Office of Science and Technology Resources, National Cancer Institute, National Institutes of Health, Bethesda, MD, USA

Abstract

Extramedullary erythropoiesis is not expected in healthy adult mice, but erythropoietic gene expression was elevated in lineage-depleted spleen cells from *cd47*$^{-/-}$ mice. Expression of several genes associated with early stages of erythropoiesis was elevated in mice lacking CD47 or its signaling ligand thrombospondin-1, consistent with previous evidence that this signaling pathway inhibits expression of multipotent stem cell transcription factors in spleen. In contrast, cells expressing markers of committed erythroid progenitors were more abundant in *cd47*$^{-/-}$ spleens but significantly depleted in *thbs1*$^{-/-}$ spleens. Single cell transcriptome and flow cytometry analyses indicated that loss of CD47 is associated with accumulation and increased proliferation in spleen of Ter119^{-}CD34^{+} progenitors and Ter119^{+}CD34^{-} committed erythroid progenitors with elevated mRNA expression of Kit, Ermap, and Tfrc. Induction of committed erythroid precursors is consistent with the known function of CD47 to limit the phagocytic removal of aged erythrocytes. Conversely, loss of thrombospondin-1 delays the turnover of aged red blood cells, which may account for the suppression of committed erythroid precursors in *thbs1*$^{-/-}$ spleens relative to basal levels in wild type mice. In addition to defining a role for CD47 to limit extramedullary erythropoiesis, these studies reveal a thrombospondin-1-dependent basal level of extramedullary erythropoiesis in adult mouse spleen.

eLife assessment

This study presents a **valuable** finding on the cell composition in mouse spleen depleted for the CD47 receptor and its signaling ligand Thrombospondin in hematopoietic differentiation. The supporting evidence is **convincing** with analytical improvements on the individual contributions of the signaling components and with functional studies. This work has implications for the role of CD47/Thsp in extramedullary erythropoiesis in mouse spleen and will be of interest to medical biologists working on cell signaling, transfusion medicine, and cell therapy.

https://doi.org/10.7554/eLife.92679.2.sa2

Introduction

CD47 is a counter-receptor for signal-regulatory protein-α (SIRPα) (Matozaki et al., 2009) and a component of a supramolecular membrane signaling complex for thrombospondin-1 that contains specific integrins, heterotrimeric G proteins, tyrosine kinase receptors, exportin-1, and ubiquilins (Gao et al., 1996; Isenberg et al., 2009; Kaur et al., 2022; Soto-Pantoja et al., 2015). CD47 binding to SIRPα on macrophages induces inhibitory signaling mediated by its cytoplasmic immunoreceptor tyrosine-based inhibition motifs that recruit and activate the tyrosine phosphatases SHP-1 and SHP-2 (Matozaki et al., 2009). Loss of this inhibitory signaling results in rapid splenic clearance of *cd47*$^{-/-}$ mouse red blood cells (RBC) when transfused into a wild type (WT) recipient (Oldenborg et al., 2000). The species-specificity of CD47/SIRPα binding constitutes a barrier to interspecies blood transfusion and hematopoietic reconstitution (Strowig et al., 2011; Wang et al., 2007).

CD47 forms nanoclusters on young RBC with limited binding to thrombospondin-1 (Wang et al., 2020). CD47 abundance decreases on aged RBCs, but CD47 on aging RBC forms larger and more dense clusters with increased ability to bind thrombospondin-1. CD47 on aging RBC also adopts an altered conformation (Burger et al., 2012). Exposure of aged RBC to thrombospondin-1 further increases the size of CD47 clusters via a lipid raft-dependent mechanism. Conversely, CD47 cluster formation was limited on *thbs1*$^{-/-}$ mouse RBC and associated with significantly increased RBC lifespan (Wang et al., 2020).

Liver and spleen are the main hematopoietic organs during embryonic development, whereas bone marrow assumes that responsibility after birth (Kim, 2010). Induction of extramedullary hematopoiesis in adult spleen can compensate for pathological conditions that compromise hematopoiesis in bone marrow (Cenariu et al., 2021). CD47 is highly expressed on proliferating erythroblasts during stress-induced erythropoiesis, and antibodies blocking either CD47 or SIRPα inhibited the required transfer of mitochondria from macrophages to developing erythroblasts in erythroblastic islands (Yang et al., 2022). Notably, treatment with a CD47 antibody enhanced splenomegaly in the anemic stress model. Consistent with the absence of inhibitory SIRPα signaling that limits clearance of aged RBC (Fossati-Jimack et al., 2002; Lutz and Bogdanova, 2013), *cd47*$^{-/-}$ mice derived using CRISPR/Cas9 exhibited hemolytic anemia and splenomegaly (Kim et al., 2018). Conversely, CD47-dependent thrombospondin-1 signaling regulates the differentiation of multipotent stem cells in a stage-specific manner (Kaur et al., 2013; Nath et al., 2018; Porpiglia et al., 2022). and both *thbs1*$^{-/-}$ and *cd47*$^{-/-}$ mouse spleens have more abundant Sox2^{+} stem cells and higher mRNA expression of the multipotent stem cell transcription factors Myc, Sox2, Oct4, and Klf4(Kaur et al., 2013). Therefore, both thrombospondin-1- and SIRPα-dependent CD47 signaling could alter erythropoiesis and contribute to spleen enlargement. Here, we utilized flow cytometry combined with bulk and single cell transcriptomics to examine extramedullary hematopoiesis in *cd47*$^{-/-}$and *thbs1*$^{-/-}$ mice, which revealed cooperative and opposing roles for CD47 and thrombospondin-1 to limit extramedullary erythropoiesis in spleen.

Results

Upregulation of erythroid precursors in *cd47*$^{-/-}$ mouse spleen

We confirmed the previously reported spleen enlargement in *cd47*$^{-/-}$ mice(Bian et al., 2016; Nath et al., 2018), but we did not observe significant spleen enlargement in *thbs1*$^{-/-}$ mice (**Figure 1–figure supplement 1A**). Enlargement of *cd47*$^{-/-}$spleens could result from increased phagocytic clearance of RBC, as reported in *cd47*$^{-/-}$ and *sirpa*$^{-/-}$mice treated with CpG (Kidder et

al., 2020) and aging *cd47*$^{-/-}$ mice (Kim et al., 2018). Alternatively, increased cell numbers could result from the increased stem cell abundance in *cd47*$^{-/-}$ spleens (Kaur et al., 2013). The spleen enlargement was associated with a significantly higher total spleen cell number in a single cell suspension after RBC lysis in *cd47*$^{-/-}$ mice compared to WT and *thbs1*$^{-/-}$ mice (**Figure 1A**).

Our previous analysis of lineage-negative cells from WT and *cd47*$^{-/-}$ spleens identified an increased abundance of NK cell precursors in *cd47*$^{-/-}$ spleens (Nath et al., 2018). Analysis of bulk RNAseq data of naïve WT and *cd47*$^{-/-}$ spleen cells depleted for proerythroblasts through mature erythrocytes using the antibody Ter-119 (Kina et al., 2000) and for cells bearing CD4, CD11b, CD11c, CD19, CD45R, CD49b, CD105, MHC Class II, and TCRγ/δ (Lin^{-}CD8^{+}) unexpectedly showed strong enrichment of a heme metabolism gene signature (**Figure 1–figure supplement 1C**), markers of stress-induced erythropoiesis (Delic et al., 2020; Thompson et al., 2010) and adult definitive erythropoiesis (Kingsley et al., 2013) in the lineage-depleted *cd47*$^{-/-}$ relative to the corresponding cells from WT spleens (**Table 1**, **Figure 1–figure supplement 1B,D**). Trim10 mRNA, which encodes an erythroid-specific RING finger protein required for terminal erythroid differentiation (Harada et al., 1999), was elevated 50-fold. Higher Mki67 mRNA expression suggested increased proliferation among Lin^{-} *cd47*$^{-/-}$ spleen cells, which also expressed elevated mRNA levels of the major erythroid transcription factor Gata1 (Gutierrez et al., 2020). Apart from increased Kit mRNA expression, however, mRNA expression of markers for multipotent erythroid progenitors including Anpep (CD13), Cd33, Sca1 and Gata2 was not elevated in the absence of CD47. These data suggested preferential accumulation of committed erythroid progenitors rather than multipotent erythroid progenitors in the *cd47*$^{-/-}$spleens. CD47 regulates activities of the nuclear transport protein exportin-1 (Kaur et al., 2022), and Xpo1 mRNA was also increased in *cd47*$^{-/-}$cells (**Table 1**). Exportin-1 is a Gata1 transcriptional target and promotes terminal erythroid differentiation by maintaining Gata1 in the nucleus (Guillem et al., 2020), which suggested a potential mechanism by which loss of CD47 could increase erythropoiesis.

To further characterize CD47-dependent spleen cells and the relevance of thrombospondin-1, single cell suspensions of depleted of mature RBC were analyzed using flow cytometry for expression of erythropoiesis-related cell surface and proliferation markers (**Figure 1B-J**, **Figure 1–figure supplement 2**). The percentages of Ter119^{+} cells in singlet cells from *cd47*$^{-/-}$ spleens was significantly higher than in WT or *thbs1*$^{-/-}$ spleens (p = 0.0061 and 0.0322 respectively, **Figure 1B**). CD34 is expressed on multipotent through the CFU-E erythroid progenitors and was expressed a significantly higher percentage on *cd47*$^{-/-}$ versus WT or *thbs1*$^{-/-}$ cells (p = 0.0008 and 0.0001 respectively, **Figure 1C**), whereas the multipotent progenitor marker Sca1 was expressed in a smaller percentage of *cd47*$^{-/-}$ versus WT or *thbs1*$^{-/-}$ spleen cells (p = 0.0001 and 0.0009 respectively, **Figure 1D**).

A higher percentage of *cd47*$^{-/-}$ cells expressed the proliferation marker Ki67 at low but not high levels compared to WT or *thbs1*$^{-/-}$ spleen cells (p = 0.0024 and 0.0003 respectively, **Figure 1E**). c-Kit signaling is crucial for normal hematopoiesis and is expressed in multipotent progenitors through CFU-E (Lennartsson and Ronnstrand, 2012; Swaminathan et al., 2022), but the percentage of cKit positive cells was higher only in *thbs1*$^{-/-}$ spleen cells (**Figure 1F**).

Erythrocyte lineage markers including Ermap, glycophorin A (Gypa), Epor and Aqp1 are established markers of stress-induced extramedullary erythropoiesis (Delic et al., 2020). The erythropoietin receptor (Epor), which is expressed in CFU-E through proerythroblasts, was expressed in significantly more *cd47*$^{-/-}$ versus WT spleen cells (p = 0.0077) but in significantly fewer *thbs1*$^{-/-}$ spleen cells (p = 0.0017 **Figure 1G**). Cells expressing the major RBC membrane glycoprotein Gypa, which accumulates in erythroblasts, Ermap, and Aqp1 showed similar significant increases in *cd47*$^{-/-}$ spleen cells, whereas only Gypa^{+} and Aqp1^{+} cells were significantly decreased in *thbs1*$^{-/-}$ spleen cells (**Figure 1H**, **I**, **J**). Consistent with their known induction kinetics, most of the cells expressing these markers were Ter119^{+}, and the alterations in their

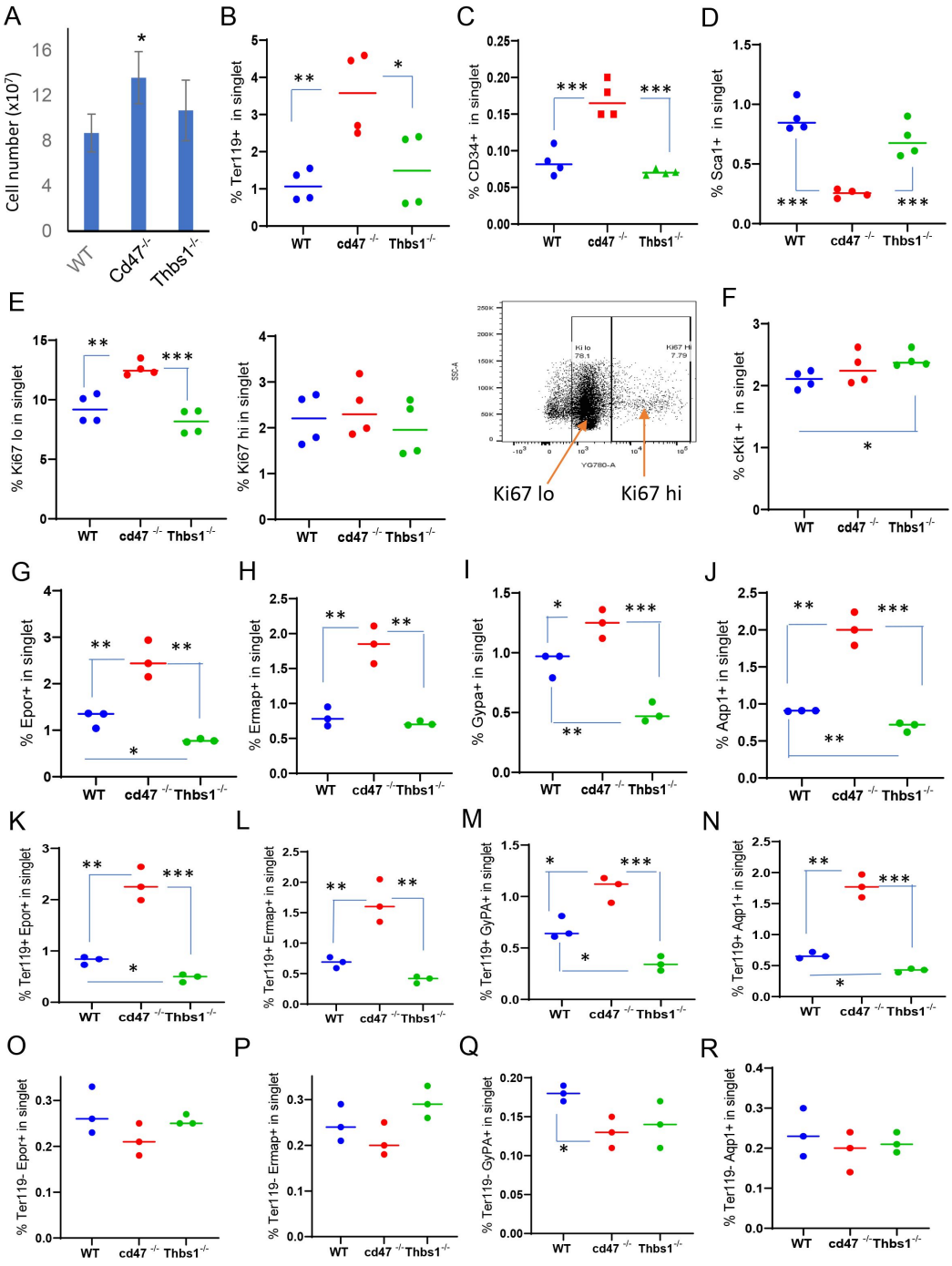

Figure 1

Effects of *Cd47* or *Thbs1* gene disruption on spleen cell numbers and content of cells expressing erythropoietic precursor markers or the proliferation marker Ki67.

(A) Total spleen cell numbers in WT, *cd47*$^{-/-}$ and *thbs1*$^{-/-}$ C57BL/6 mice determined after lysis of RBC (mean±SEM, n =3). Flow cytometry was performed to analyze gated singlet spleen cells stained with Ter119 antibody (B), CD34 antibody (C), Sca1 antibody (D), Ki67 antibody with the indicated gating for high and low expression (E), cKit antibody (F), Epor antibody (G), Ermap antibody (H), Gypa antibody (I), or Aqp1 antibody (J). Further analysis of Epor (K,O), Ermap (L,P), Gypa (M,Q), and Aqp1 expression (N,R) was performed after gating for Ter119 expression. The percentages of cells positive for the indicated surface markers are presented (n = 3 or 4). P-values were determined using a two-tailed t test for two-samples assuming equal variances in GraphPad Prism. * = p<0.05, ** = p<0.01, *** = p<0.001

Gene	Erythropoiesis expression/function	Fold change *cd47*$^{-/-}$/*WT*[a]	T Statistic	P-Value
Ermap	extramedullary erythropoiesis marker[b]	21.5	6.04	$9.35x10^{-5}$
Tal1	extramedullary erythropoiesis marker[b]	13.9	5.13	$3.55x10^{-4}$
Gypa	extramedullary erythropoiesis marker[b]	89.3	3.67	$3.86x10^{-3}$
Gata1	extramedullary erythropoiesis marker[b]	7.69	4.86	$5.38x10^{-4}$
Kel	extramedullary erythropoiesis marker[b]	29.0	4.61	$8.04x10^{-4}$
Slc4a1	extramedullary erythropoiesis marker[b]	151.4	4.90	$5.05x10^{-4}$
Klf1	extramedullary erythropoiesis marker[b]	20.6	5.06	$3.95x10^{-4}$
Cldn13	extramedullary erythropoiesis marker[b]	49.2	4.42	$1.09\ x10^{-3}$
Trim10	extramedullary erythropoiesis marker[b]	49.7	4.11	$1.83\ x10^{-3}$
Epor	extramedullary erythropoiesis marker[b]	12.3	4.91	$5.01x10^{-4}$
Sptb	extramedullary erythropoiesis marker[b]	36.5	5.21	$3.16x10^{-4}$
Rhag	extramedullary erythropoiesis marker[b]	33.0	4.64	$7.68x10^{-4}$
Hba-a1	erythroblasts	63.8	6.46	$5.23x10^{-5}$
Hbb-bs	erythroblasts	59.2	6.60	$4.34x10^{-5}$
Gata1	BFU-E through erythroblasts	7.69	4.86	$5.38x10^{-4}$
***Tfrc* (CD71)**	CFU-E through erythroblasts	3.12	6.19	$7.58x10^{-5}$
Kit	Progenitors through CFU-E	1.72	6.24	$7.02x10^{-5}$
Sox6	Adult definitive erythropoiesis	35.5	3.56	0.0046
Aqp1	Adult definitive erythropoiesis	26.9	6.51	$4.91x10^{-5}$
Nr3c1	Adult definitive erythropoiesis	1.12	2.80	0.018
Mki67	Proliferation marker	4.43	7.65	$1.14x10^{-5}$
Cd34	Multipotent progenitors through CFU-E	1.60	1.59	0.141
***Ly6a* (Sca1)**	Multipotent progenitors	1.17	1.02	0.331
***Anpep* (CD13)**	Multipotent progenitors	1.16	1.14	0.28
Cd33	Multipotent progenitors	-1.06	-0.37	0.71
Gata2	Multipotent progenitors	1.08	0.66	0.52
Xpo1	Stability of nuclear Gata1	1.23	3.86	$2.7x10^{-3}$

[a]Gene enrichment in naïve *cd47*$^{-/-}$ vs WT spleen cells depleted for CD4, CD11b, CD11c, CD19, CD45R (B220), CD49b (DX5), CD105, MHC Class II, Ter-119, and TCRγ/δ.

[b]Reported markers of stress-induced extramedullary erythropoiesis (Delic et al., 2020; Thompson et al., 2010)

Table 1.

Expression of erythropoiesis-associated genes in lineage-depleted *cd47*$^{-/-}$ versus WT spleen cells

abundance observed in *cd47*$^{-/-}$and *thbs1*$^{-/-}$ spleens were restricted to Ter119^{+} cells (**Figure 1K-R**). These results indicate an increased abundance of committed erythroid progenitors spanning CD34^{+} progenitors through reticulocytes in the *cd47*$^{-/-}$ spleen but depletion of the earlier Sca1^{+} multipotent progenitors. Consistent with the decreased turnover of *thbs1*$^{-/-}$ RBC (Wang et al., 2020), cells expressing the committed erythroid markers Gypa, Epor, and Aqp1 were depleted in *thbs1*$^{-/-}$ spleens.

Erythropoietin binding to Epor on early erythroid precursor cells stimulates their survival, proliferation, and differentiation by inducing the master transcriptional regulators Tal1, Gata1, and Klf1 (Perreault and Venters, 2018). Tal1, Gata1, and Klf1, and Epor mRNAs were strongly up-regulated in *cd47*$^{-/-}$ relative to WT spleens (**Table 1**). The increased proliferative response in the *cd47*$^{-/-}$ cells is consistent with a significant increase in Epor^{+} Ter119^{+} *cd47*$^{-/-}$ cells, contrasting with a significant decrease in their abundance in Ter119^{+} *thbs1*$^{-/-}$ cells (**Figure 1K**). Epor expression was minimal and unchanged in the Ter119^{-} population (**Figure 1O**), indicating that the Ter119 antigen is expressed in erythroid precursors that are responsive to erythropoietin. These data are consistent with increased extramedullary erythropoiesis in *cd47*$^{-/-}$ and suppressed extramedullary erythropoiesis relative to WT in *thbs1*$^{-/-}$ spleens.

CD47-dependence of erythropoietic markers in Ter119^{+} and Ter119^{-} cells

The Ter119 antibody recognizes an antigen highly expressed in mouse proerythroblasts through mature erythrocytes (Kina et al., 2000). Although Ter119 is a widely used erythroid lineage marker, its epitope does not map to a specific protein (Kina et al., 2000) and requires 9-O-acetylation of sialic acids that are present on several RBC glycoproteins (Mahajan et al., 2019). Although no effect of CD47 on the abundance of cKit^{+} cells was detected (**Figure 1F**), Kit mRNA was significantly enriched in lineage-negative *cd47*$^{-/-}$ spleen cells (**Table 1**). To resolve this discrepancy, the percentage of cKit^{+} cells was assessed in Ter119^{+} and Ter119^{-} populations (**Figure 2A**, **Figure 2–figure supplement 1**). A higher percentage of the cd*47*$^{-/-}$ cells were Ter119^{+}cKit^{+}. Consistent with **Figure 1F** and the elevation of multipotent stem cells in *thbs1*$^{-/-}$ spleen (Kaur et al., 2013), Ter119^{-}cKit+ cells were elevated in *thbs1*$^{-/-}$ spleens. Consistent with the bulk RNA sequencing data, Sca1^{+} cells in spleen did not differ in the Ter119^{+} cells and were less abundant in Ter119^{-} cells from *cd47*$^{-/-}$ spleens relative to the same subset from WT (**Figure 2B**). Consistent with the negative regulation of stem cell transcription factors in spleen by CD47-dependent thrombospondin-1 signaling (Kaur et al., 2013), these results support prior evidence that that loss of *thbs1* or *cd47* results in accumulation of early hematopoietic precursors that are Ter119^{-} and demonstrates a *cd47*$^{-/-}$-specific enrichment of cKit^{+}Ter119^{+} committed erythroid precursors. Proliferating cells with low Ki67 expression were more abundant in the Ter119^{+} and Ter119^{-} populations of *cd47*$^{-/-}$ cells relative to WT and *thbs1*$^{-/-}$cells, suggesting that loss of *cd47* but not *thbs1* increases the proliferation of committed erythroid precursors (**Figure 2C**, D).

CD47 limits proliferation of Ter119^{+}CD34^{-} and Ter119^{-}CD34^{+} spleen cells

Although **Figure 1** demonstrated increased numbers of Ter119^{+} and CD34^{+} cells in *cd47*$^{-/-}$ spleens, further analysis revealed that more CD34^{+} cells are Ter119^{-} than Ter119^{+} (**Figure 2E,G** left panels). Therefore, loss of CD47 upregulates both early Ter119^{-}CD34^{+} progenitors and more mature Ter119^{+} progenitors, most of which have lost CD34 expression (**Figure 2F**). Most of the increased proliferation of *cd47*$^{-/-}$ spleen cells, indicated by Ki67 expression, was in the Ter119^{+}CD34^{-} subset (**Figure 2F**, center and right panels), but proliferating *cd47*$^{-/-}$ cells were also enriched in the Ter119^{-}CD34^{+} population (**Figure 2G**). These data indicate roles for more differentiated Ter119^{+}/CD34^{-} erythroid progenitors as well as earlier Ter119^{-}/CD34^{+} erythroid progenitors in mediating the increased extramedullary erythropoiesis in *cd47*$^{-/-}$ spleens.

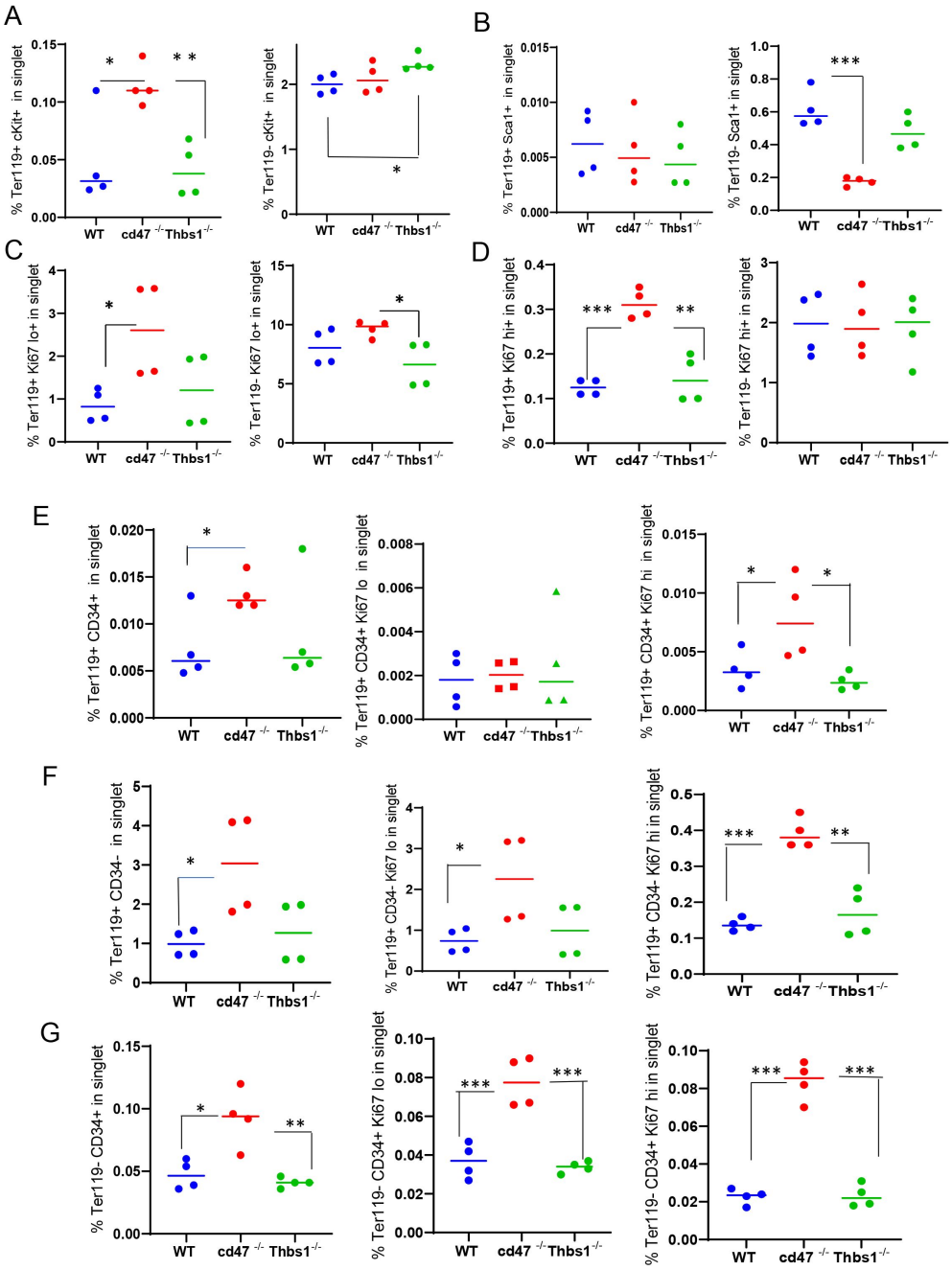

Figure 2

Effects of *Cd47* or *Thbs1* gene disruption on the percentage of Ter119$^+$ and Ter119$^-$ spleen cells expressing markers of multipotent and committed erythroid precursors and cell proliferation.

Spleen cells isolated from WT, *cd47*$^{-/-}$and *thbs1*$^{-/-}$ mice were costained with Ter119 antibody along with cKit, Ki67, Sca1 Ermap, Gypa, Epor or Aqp1 antibodies and acquired on an LSRFortessa SORP. After gating for singlet cells, the percentages of Ter119$^+$ and Ter119$^-$ cells positive for stem cell markers cKit (A) and Sca1 (B), high or low levels of the proliferation marker Ki67 (C,D), were compared among WT, *cd47*$^{-/-}$ and *thbs1*$^{-/-}$ mouse spleens (n = 3-4). The proliferation of CD34$^+$ and CD34$^-$ populations of Ter119$^+$ spleen cells from WT, *cd47*$^{-/-}$, *thbs1*$^{-/-}$ mice was evaluated by staining with CD34, Ter119 and Ki67 antibodies. Ter119$^+$CD34$^+$ cells (E), Ter119$^+$CD34$^-$ cells (F), and Ter119$^-$CD34$^+$ cells (G) were also quantified (left panels) and analyzed for the proliferation marker Ki67 (center and right panels). P-values were determined using a two-tailed t test for two-samples assuming equal variances in GraphPad Prism. * = p<0.05, ** = p<0.01, *** = p<0.001

Identification of CD47-dependent erythroid precursor populations

Single cell RNA sequencing (scRNAseq) was used to further define effects of CD47 and thrombospondin-1 on erythroid precursors in spleen (**Figure 3**, **Figure 3–figure supplement 1**). Spleen cells from WT, *cd47*$^{-/-}$ and *thbs1*$^{-/-}$ mice were treated with immobilized antibodies to deplete monocytic, T, B, and NK cell lineages and mature RBC and subjected to scRNAseq analysis. Following alignment, the mRNA expression data were clustered in two dimensions using the t-distributed stochastic neighbor embedding (tSNE) method in NIDAP. Using a resolution of 0.4, the spleen cells clustered in 18 groups (**Figure 3A**).

Cell type analysis using SingleR with Immgen and mouse RNAseq databases identified the main cell types in each cluster (**Figure 3B**). Immgen main cell type annotation identified cluster 12 and a subset of cluster 14 as stem cells, and mouse RNA seq annotation identified erythrocyte signatures mostly in cluster 12. WT, *cd47*$^{-/-}$ and *thbs1*$^{-/-}$ cells clustered by genotype in the major residual T cell clusters 0 through 5 but had similar distributions within clusters 12 and 14 (**Figure 3C,D**).

Erythroid lineage markers were found mainly in cluster 12, which contained 440 cells (**Figure 4** and **Figure 4–figure supplement 1**, **2**). Consistent with the flow data in **figures 1** and 2, *cd47*$^{-/-}$cells were more abundant in cluster 12 (65%), and *thbs1*$^{-/-}$ cells were less abundant (15%) than WT cells (21%). CD34 was expressed mostly in cluster 14 and to lower parts of cluster 12, whereas Ly6a (Sca1) was restricted to isolated cells in both clusters. Kit and Gata2, which are expressed by multipotent progenitors through CFU-E, were expressed in lower and middle areas of cluster 12 and to a limited degree in cluster 14 (**Figure 4**). The extramedullary erythropoiesis markers Epor, Gata1, Klf1, and Ermap, the definitive erythropoiesis marker Aqp1 and the proliferation marker Ki67 had similar distributions in cluster 12 (**Figure 4**). Trim10 and the late erythroid markers Gypa, Tmem56, Epb42, Spta1, and Sptb were restricted to the upper regions of cluster 12 (**Figure 4**). Therefore, erythroid differentiation within cluster 12 correlates with increasing TSNE-2 scores.

Similar high percentages of WT and *cd47*$^{-/-}$ cells within cluster 12 expressed the erythroid lineage markers Klf1, Aqp1, Epor, Ermap, and Gata1, but percentages for Klf1, Epor, and Gata1 were lower in *thbs1*$^{-/-}$ cells (**Figure 4–figure supplement 3A**). Expression of the erythroid genes *Klf1, Aqp1, Epor*, *Ermap,* and *Gata1* was not detected in the stem cell cluster 14 (**Figure 4–figure supplement 3A**). The average mRNA/cell for Tfrc and Ermap was significantly higher in *cd47*$^{-/-}$ cells, whereas mRNAs encoding Klf1, Aqp1, Epor, and Gata1 were significantly lower in *thbs1*$^{-/-}$ cells compared to WT (**Figure 5A**, **Table 2**). Violin plots indicated that cells with the highest Mki67 mRNA expression were more abundant in *cd47*$^{-/-}$ cells in cluster 12, and the average expression was higher ($p=9.2x10^{-6}$), but cells with high and low Mki67 had similar distributions in *thbs1*$^{-/-}$ and WT cells (**Figure 5A**). Mki67 expression levels were lower in cluster 14, and *cd47*$^{-/-}$ cells had higher mean expression that WT, but *thbs1*$^{-/-}$ cells had lower Mki67 expression than WT (**Table 2**). Expression of Kit was also higher in *cd47*$^{-/-}$ versus WT cells in cluster 12 (p=0.0015). Although more *cd47*$^{-/-}$ cells expressed Gata1 and Epor, their mean expression was not higher than in WT cells.

Expression of Xpo1 and Ranbp2, which regulates activity of the Xpo1/Ran complex that stabilizes Gata1 (Ritterhoff et al., 2016), was higher in cluster 12 than in cluster 14, and within cluster 12 the distribution of positive cells was similar to that for other markers of committed erythroid precursors (**Figure 4**). The average Xpo1 expression in cluster 12 was significantly higher in *cd47*$^{-/-}$ and *thbs1*$^{-/-}$ cells compared to WT, whereas expression was not *Cd47*- or *Thbs1*-dependent in cluster 14 (**Figure 5A,B**, **Table 2**).

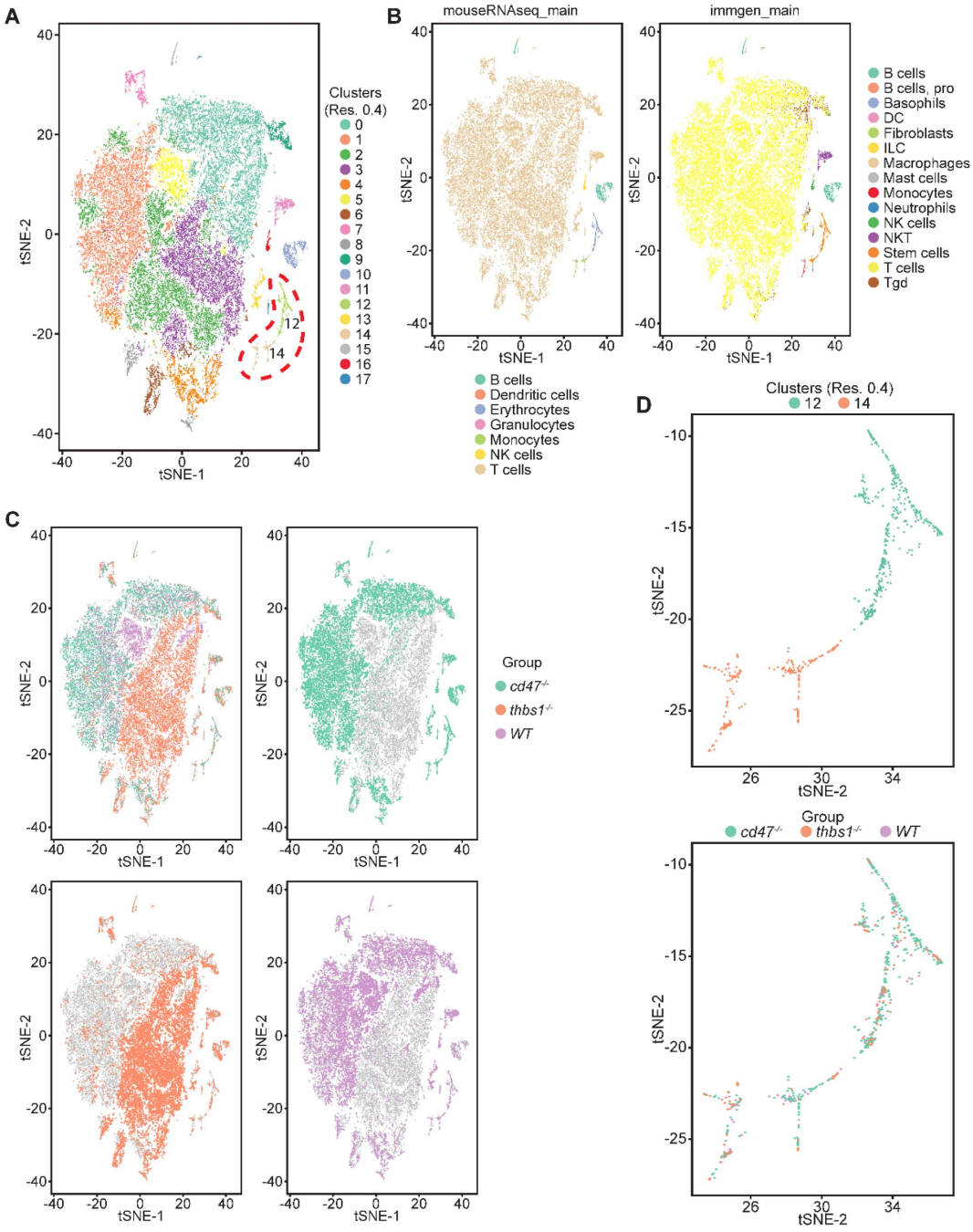

Figure 3

Effects of *cd47* and *thbs1* gene deletion on stem cell and erythroid precursor populations in mouse spleen identified using single cell RNA sequence analysis.

(A) tSNE clustering analysis of lineage-depleted spleen cells from WT, *cd47*$^{-/-}$ and *thbs1*$^{-/-}$mice. The encircled area contains erythroid cells (clusters 12) and stem cells (cluster 14). (B) Cell type analysis using Immgen and Mouse RNAseq and SingleR (v.1.0) databases. (C) Distribution of WT, *cd47*$^{-/-}$ and *thbs1*$^{-/-}$spleen cells in each cluster of the tSNE plot. (D) Enlarged plots of clusters 12 and 14 and cells in these clusters colored by genotype.

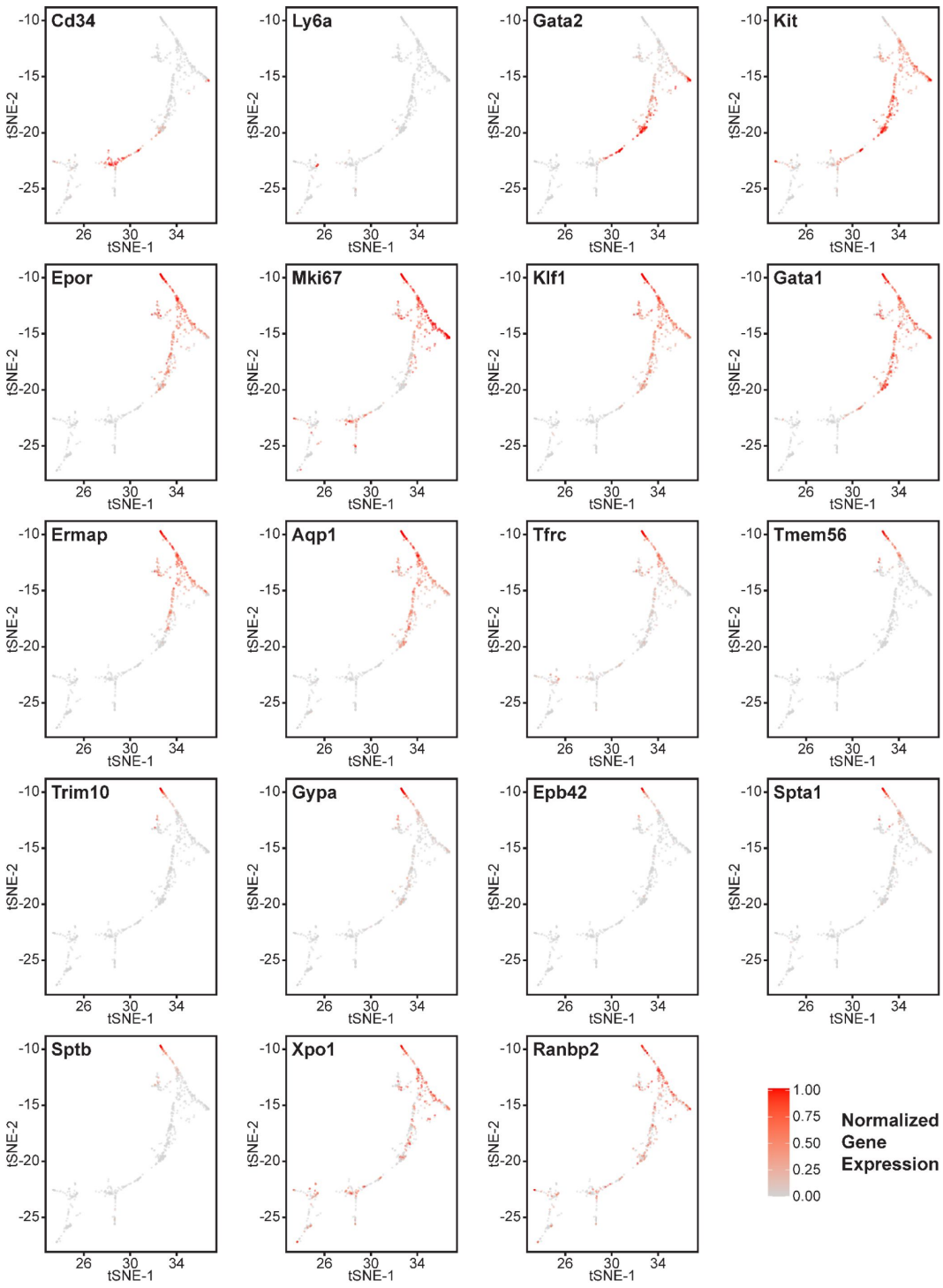

Figure 4

Effects of *cd47* and *thbs1* gene deletion on gene expression in stem cell and erythroid precursor clusters.

High resolution tSNE plots showing the distribution of mRNAs encoding the multipotent stem cell markers CD34 and Ly6a (Sca1) and Gata2, the erythropoietic markers Kit and Epor, the proliferation marker Mki67, erythroid differentiation transcription factors Klf1 and Gata1, and erythroid differentiation and extramedullary erythropoiesis markers Ermap, Aqp1, Tmem56, Trim10, Gypa1, Spta1, Sptb, Ebp42, Xpo1, and RanBP2 in clusters 12 and 14. Expression levels were normalized to maximum expression of each mRNA in these clusters.

		Cd47$^{-/-}$ vs WT		*Thbs1*$^{-/-}$ vs WT	
Cluster	**Gene**	**p-value**	**Avg log_2 FC**	**p-value**	**Avg log_2 FC**
12	*Klf1*	0.463	-0.115	0.0023	-0.510
12	*Aqp1*	0.331	-0.130	0.0011	-0.472
12	*Tfrc*	0.017	0.531	0.93	0.009
14	*Tfrc*	0.64	0.071	0.922	0.016
12	*Epor*	0.506	-0.078	$4.75x10^{-5}$	-0.576
12	*Ermap*	$5.1x10^{-3}$	0.309	0.65	-0.073
12	*Gata1*	0.57	0.007	0.0011	-0.377
12	*Mki67*	$9.16x10^{-6}$	0.997	0.22	0.456
14	*Mki67*	0.0089	0.798	0.0017	-0.062
12	*Kit*	0.0015	0.331	0.057	0.264
14	*Kit*	0.020	0.409	0.58	0.222
12	*Xpo1*	$3.31x10^{-8}$	0.472	0.0069	0.323
14	*Xpo1*	0.079	0.211	0.19	0.148
12	*Ranbp1*	0.24	0.108	0.13	0.079
14	*Ranbp1*	0.91	0.069	0.076	-0.486
12	*Ranbp2*	$1.98x10^{-14}$	0.754	0.092	0.269
14	*Ranbp2*	0.0056	0.365	0.88	0.042
12	*Nr3c1*	$8.5x10^{-4}$	0.320	$8.8x10^{-4}$	0.430
14	*Nr3c1*	0.012	0.153	$8.6x10^{-5}$	0.428
12	*Ddx46*	$3.04x10^{-8}$	0.530	$2.68x10^{-10}$	0.779
14	*Ddx46*	0.0014	0.385	0.0023	0.490

Table 2.

Differential mRNA expression of erythropoietic, stem cell, and proliferation associated markers in WT, *cd47*$^{-/-}$, and *thbs1*$^{-/-}$ cells in clusters 12 and 14.

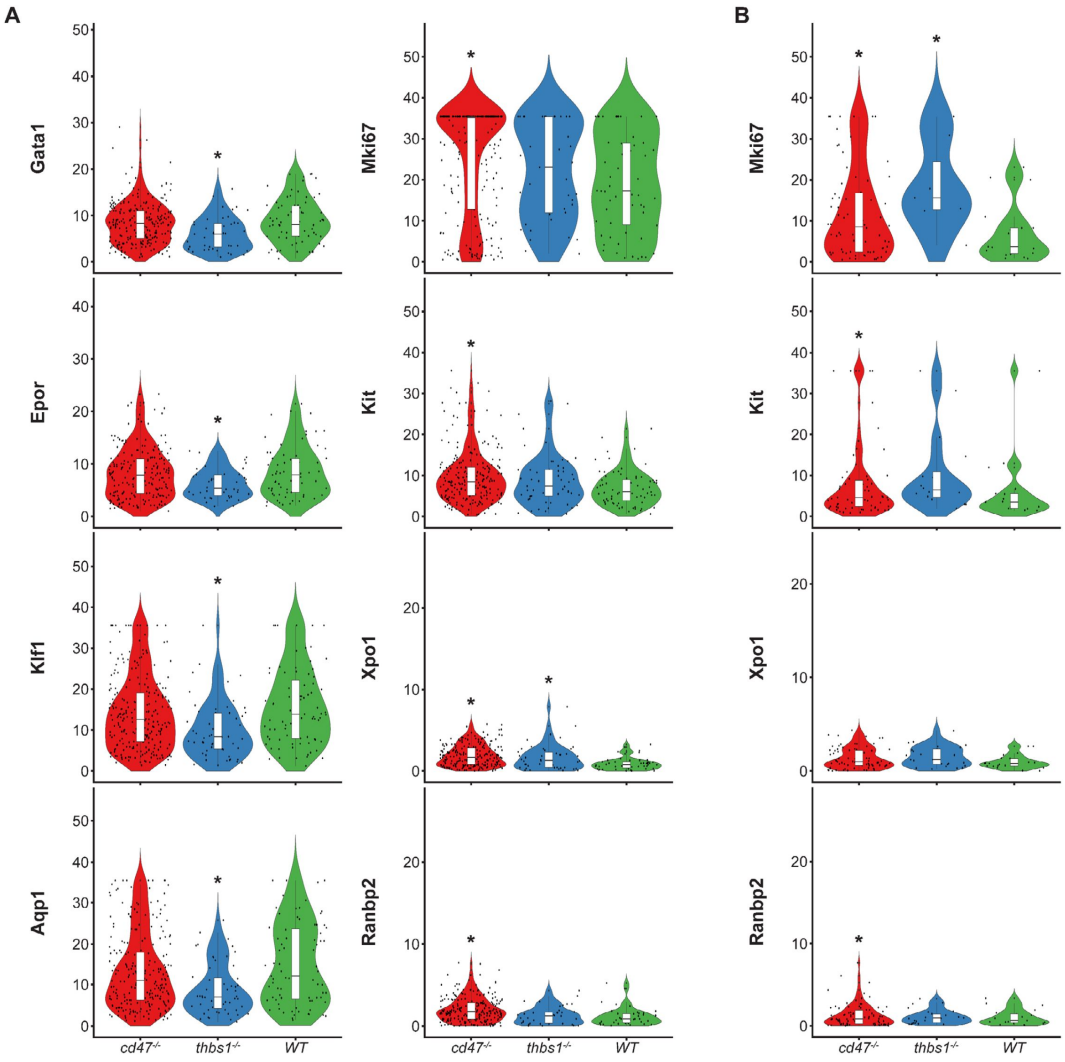

Figure 5.

Differential effects of *cd47* and *thbs1* gene deletion on mRNA expression levels in erythroid precursor and stem cell clusters 12 and 14.

(A) Violin plots comparing mRNA expression levels of the indicated genes in *cd47*$^{-/-}$(red), *thbs1*$^{-/-}$(blue) and WT spleen cells (green) in cluster 12. (B) Violin plots comparing mRNA expression levels of the indicated genes in *cd47*$^{-/-}$, *thbs1*$^{-/-}$ and WT spleen cells in cluster 14. * = p<0.05 relative to WT cells in the respective cluster.

Resolution of cluster 12 into $CD34^+$ and $CD34^-$ cells revealed that the CD47-dependent expression of Xpo1 and Ranbp2 was restricted to the $CD34^-$ population (**Figure 4–figure supplement 3B**). Xpo1 was also *Thbs1*-dependent in the $CD34^-$ cells but could not be evaluated in $CD34^+$ due to lack of an adequate $thbs1^{-/-}$ cell number. In contrast, expression of mRNA for RanBP1, which regulates the physical interaction of Xpo1 with CD47 (Kaur et al., 2022), did not differ in $cd47^{-/-}$ or $thbs1^{-/-}$ cells in clusters 12 (**Table 2**). Nr3c1, a marker of adult definitive erythropoiesis (Kingsley et al., 2013), and Ddx46, which is required for hematopoietic stem cell differentiation (Hirabayashi et al., 2013), were among the genes with increased percentages of positive cells and significantly increased average expression in both $cd47^{-/-}$ and $thbs1^{-/-}$ cells in cluster 12 (**Figure 4–figure supplement 3A**, **Table 2**). These genes also showed CD47-dependent expression in cluster 14, but with less significant p-values for expression per cell (**Table 2**).

The co-expression of mRNAs for erythropoietic genes was compared in cluster 12 cells from $cd47^{-/-}$, WT, and $thbs1^{-/-}$ spleens (**Table 3**). Small fractions of the WT $CD34^+$ cells expressed Gata1 and Klf1 mRNAs, 2.2% expressed Mki67, and none expressed Ermap. Consistent with the flow cytometry data in **Figure 2**, coexpression of the respective genes with CD34 was more frequent in $cd47^{-/-}$ cells in cluster 12, but generally less in $thbs1^{-/-}$ cells. Notably, $CD34^+$ $thbs1^{-/-}$ cells showed no Mki67 coexpression. In contrast, WT cells that expressed committed erythroid differential markers were highly proliferative. Coexpression of all these genes with Mik67 was more frequent in $cd47^{-/-}$ cells compared to WT cells, but only for Kit and Ly6a in $thbs1^{-/-}$ cells. Coexpression of the erythroid transcription factors Gata1 and Klf1 was similarly increased in $cd47^{-/-}$ cells but decreased in $thbs1^{-/-}$ cells compared to the WT cells in cluster 12. The latter is consistent with the extended life span of $thbs1^{-/-}$ RBC (Wang et al., 2020). Kit coexpression with the erythroid lineage markers Ermap and Klf1 was moderately dependent on genotype, and Ly6a coexpression with these markers was decreased for $cd47^{-/-}$ cells in cluster 12.

A report that CD47 mediates transfer of mitochondria from macrophages to early erythroblasts during stress-induced erythropoiesis suggested that erythroid precursors in $cd47^{-/-}$ mice would have lower expression of mitochondrial chromosome-encoded genes (Yang et al., 2022). However, *mt-Atp8*, *mt-Nd3*, *mt-Nd4l*, *mt-Nd5*, and *mt-Nd6* were among the most significantly up-regulated genes in $cd47^{-/-}$ cells in cluster 12 (**Figure 4–figure supplement 3C**). Consistent with CD47 and TSP1 regulation of mitochondrial homeostasis in other cell types (Frazier et al., 2011; Kelm et al., 2020; Miller et al., 2015; Norman-Burgdolf et al., 2020), expression of *mt-Atp8*, *mt-Nd4l*, *mt-Nd5*, and *mt-Nd6* was also increased in $thbs1^{-/-}$ cells in cluster 12. However, expression of other mitochondrial-encoded genes was significantly decreased in $thbs1^{-/-}$ cells in cluster 12.

Reclustering and analysis of cells expressing erythroid signature genes

Erythrocyte progenitor markers were expressed mainly within cluster 12, but some positive cells were scattered across the T cell clusters 0 through 5 (**Figure 6A**, **Figure 6–figure supplement 1A**). To determine whether the latter positive cells include relevant erythroid lineages that were missed in the initial clustering, five lineage markers Gypa, Ermap, Klf1, Gata1, and Aqp1 that predominately localized in cluster 12 (**Figure 6–figure supplement 1A**) were selected as an erythroid signature to calculate module scores (**Figure 6–figure supplement 1A,B**). The 1007 cells that express this signature based on module scores (**Figure 6A**) were then reclustered, yielding 5 clusters within two major clusters in a UMAP projection (**Figure 6B**). Immgen annotations predicted that the major clusters represent T cells (548 cells) and stem cells (419 cells, **Figure 6C**). Mouse RNAseq annotation confirmed the T cell cluster and predicted the stem cell cluster to be of erythrocyte lineage (**Figure 6C**). WT, $cd47^{-/-}$ and $thbs1^{-/-}$ cells were uniformly distributed throughout the erythroid cluster but segregated within the T cell cluster (**Figure 6D**). $Cd47^{-/-}$ cells were more abundant in the erythroid cluster (271 cells) and $thbs1^{-/-}$ cells were less abundant (58 cells) relative to WT cells (90 cells).

Cluster 12 gene coexpression	WT	*Cd47*$^{-/-}$	*Thbs1*$^{-/-}$
Cd34_Ermap	0.0%	1.8%	1.6%
Cd34_Klf1	6.5%	8.1%	3.1%
Cd34_Gata1	6.5%	8.4%	0.0%
Mki67_Cd34	2.2%	6.3%	0.0%
Mki67_Ermap	55.4%	63.0%	54.7%
Mki67_Kit	48.9%	67.2%	57.8%
Mki67_Ly6a	37.0%	48.2%	43.8%
Mki67_Klf1	62.0%	74.6%	57.8%
Mki67_Epor	54.4%	62.7%	53.1%
Klf1_Ermap	67.4%	68.0%	62.5%
Klf1_Gata1	78.3%	82.4%	59.4%
Ermap_Gata1	62.0%	65.1%	56.2%
Kit_Ermap	54.4%	56.7%	59.4%
Kit_Klf1	71.7%	77.1%	78.1%
Ly6a_Ermap	42.4%	37.7%	46.9%
Ly6a_Klf1	64.1%	59.2%	67.2%

Table 3.

Co-expression of the indicated erythropoiesis related genes in WT, *cd47*$^{-/-}$ and *thbs1*$^{-/-}$ spleen cells in cluster 12 was quantified and expressed as a percentage of the total cell number of each genotype in cluster 12.

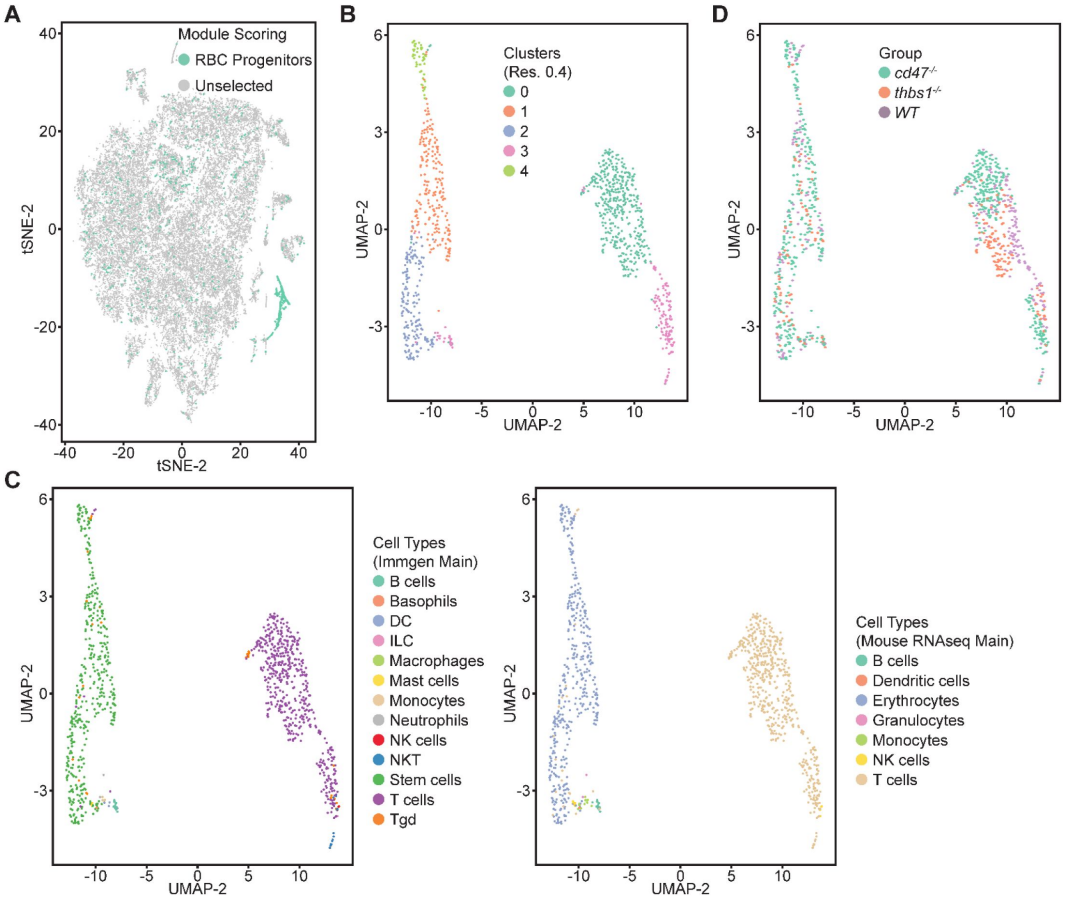

Figure 6.

Re-clustering of lineage-depleted spleen cells selected for expression of erythroid signature genes.

(A) tSNE plot showing the distribution of cells selected for expressing threshold levels of Gypa, Ermap, Klf1, Gata1, and/or Aqp1. (B) Re-clustered cells expressing the erythroid progenitor signature are displayed in a UMAP projection. (C) Immgen and mouse RNAseq main cell type annotation of reclustered cells expressing the erythroid gene signature. (D) Distribution of WT (purple), *cd47*$^{-/-}$ (green), and *thbs1*$^{-/-}$ cells (orange) in the erythroid precursor and T cell clusters.

A volcano plot indicated major differences in the transcriptomes of the two main clusters consistent with their respective erythroid and T cell lineages (**Figure 6–figure supplement 1C**). The expression of Ermap, Klf1, and Aqp1 mRNAs in 20-30% of cells in the T cell cluster is consistent with previous reports of their expression in minor subsets of T cells (Moon et al., 2004; Su et al., 2021; Teruya et al., 2018) (**Figure 7**, **Figure 7–figure supplement 1**).

The distribution of erythroid markers throughout the reclustered erythroid population was consistent with the results for cluster 12 (**Figure 7**). $CD34^+$ cells were concentrated in the lower region of the erythroid cell cluster. Consistent with the selection of cells based on expression of committed erythroid lineage genes, the cluster lacked $Ly6a^+$ cells. Kit was expressed by the $CD34^+$ cells and extended upward through the cluster. The upper cells showed increased expression of Epor, Klf1, Gata1, and Aqp1. Expression of the proliferation marker Mki67 was strongest in the upper region of the erythroid cell cluster and extended to cells that cells that expressed markers of more mature precursors including Ermap, Tfrc (transferrin receptor), and Tmem56. Trim10 mediates terminal erythroid differentiation and colocalized with mRNAs encoding glycophorin A, spectrin A, spectrin B, and band 4.2. The upregulation of erythrocyte lineage markers coincided with more abundant *cd47*$^{-/-}$ cells in this cluster, which supports the initial unsupervised clustering and confirms increased extramedullary erythropoiesis in *cd47*$^{-/-}$ mice.

Differential gene expression analysis contrasting *cd47*$^{-/-}$and *thbs1*$^{-/-}$ with WT cells in the erythroid cluster (**Table 4**) reproduced all of the results found in cluster 12 (**Table 2**). Mki67, Tfrc and Ermap mRNAs were significantly higher in *cd47*$^{-/-}$cells compared to WT, whereas Klf1, Aqp1, Epor, and Gata1 mRNAs were significantly lower in *thbs1*$^{-/-}$ cells (**Table 4**).

Differences in the percentages of cells expressing these genes seen in cluster 12 were also reproduced in the reclustered erythroid cells (**Figure 7–figure supplement 1**). The altered expression of Xpo1 and RanBP2 were also confirmed in the erythroid cluster, but Xpo1 mRNA expression was not CD47-dependent in the T cell cluster (**Table 4**). Notably, the increased expression of Nr3c1, and Ddx46 mRNAs in *cd47*$^{-/-}$ and *thbs1*$^{-/-}$ cells in the erythroid cell cluster was also found in the reclustered T cells (**Table 4**). However, the T cell cluster completely lacked expression of the proliferation-associated markers Mki67 and Tfrc. Aqp1 and Gata1were also expressed by a subset of the T cells (**Figure 7–figure supplement 1**), but their decreased expression in *thbs1*$^{-/-}$ cells was not seen in the T cell cluster (**Table 4**).

Discussion

Our data supports a role for thrombospondin-1-stimulated CD47 signaling to limit early stages of erythropoiesis in WT mouse spleen and opposing roles for thrombospondin-1 and CD47 to regulate SIRPα-dependent turnover of RBC. The increased anemic stress in *cd47*$^{-/-}$ spleen increases extramedullary erythropoiesis, whereas extramedullary erythropoiesis is suppressed by the decreased RBC turnover in *thbs1*$^{-/-}$ spleen. These studies are consistent with the reported increased red cell turnover in *cd47*$^{-/-}$ mice and decreased RBC turnover in *thbs1*$^{-/-}$mice compared to WT mice (Wang et al., 2020). Increased RBC clearance in *cd47*$^{-/-}$ mice is mediated by loss of the “don’t eat me” function of CD47 on red cells (Kim et al., 2018; Oldenborg et al., 2000). In wildtype mice, clearance is augmented by thrombospondin-1 binding to the clustered CD47 on aging red cells (Wang et al., 2020). Thus, anemic stress in the mouse strains studied here and the abundance of committed erythroid progenitors in their spleens decrease in the order *cd47*$^{-/-}$> WT > *thbs1*$^{-/-}$.

Independent of CD47 protecting erythropoietic cells from phagocytosis, we previously found that bone marrow from *cd47*$^{-/-}$ mice subjected to the stress of ionizing radiation exhibited more colony forming units for erythroid (CFU-E) and burst-forming unit-erythroid (BFU-E) progenitors compared to bone marrow from irradiated wildtype mice (Maxhimer et al., 2009). Loss of CD47

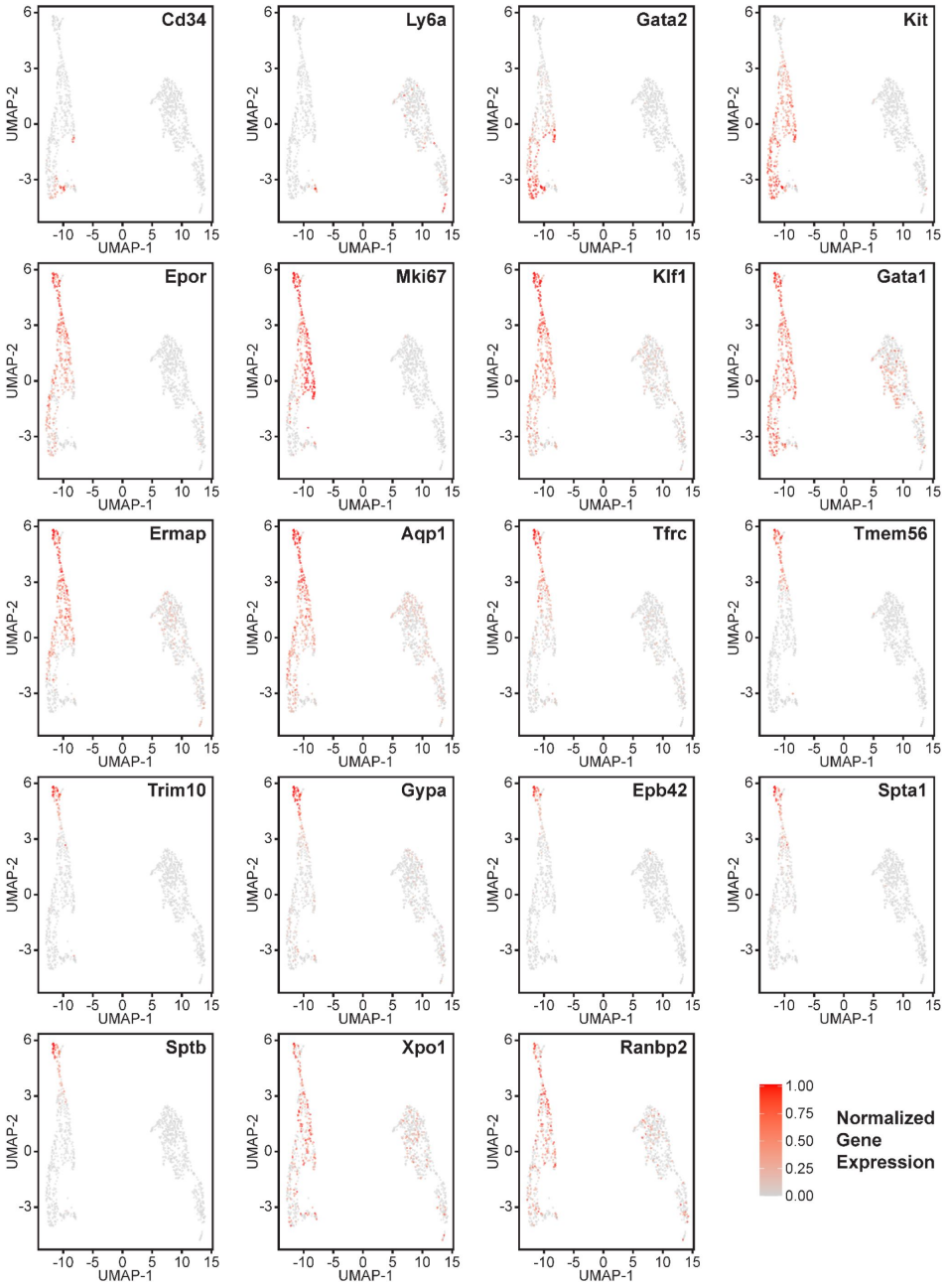

Figure 7.

Gene expression in reclustered lineage-depleted spleen cells selected for expression of erythroid signature genes.

Distribution of the multipotent stem cell markers CD34 and Ly6a (Sca1), erythropoietic markers Gata2, Kit and Epor, the erythroid differentiation transcription factors Klf1 and Gata1, and erythroid differentiation and extramedullary erythropoiesis marker the proliferation marker Mik67, and the erythroid markers Ermap, Tfrc, Aqp1, Tfrc, Tmem56, Trim10, Gypa1, Ebp42, Spta1, Sptb, Xpo1 and Ranbp2 in the erythroid lineage cluster (left) and T cell cluster (right). Expression levels were normalized to maximum expression of each mRNA in these clusters.

		Cd47$^{-/-}$ vs WT		*Thbs1*$^{-/-}$ vs WT	
Cluster	**Gene**	**p-value**	**Avg log_2 FC**	**p-value**	**Avg log_2 FC**
Erythroid	*Klf1*	0.507	-0.095	0.0016	-0.526
Erythroid	*Aqp1*	0.196	-0.088	$8.1x10^{-4}$	-0.390
T cells	*Aqp1*	0.662	0.027	0.350	-0.092
Erythroid	*Tfrc*	0.015	0.549	0.936	0.054
T cells	*Tfrc*	-	-	-	-
Erythroid	*Epor*	0.767	-0.046	0.026	-0.219
Erythroid	*Ermap*	0.0064	0.326	0.496	-0.010
T cells	*Ermap*	0.335	0.076	0.697	0.063
Erythroid	*Gata1*	0.38	0.009	0.0040	-0.337
T cells	*Gata1*	0.0044	-.0.162	0.302	0.093
Erythroid	*Mki67*	$4.6x10^{-6}$	1.015	0.118	0.545
T cells	*Mki67*	-	-	-	-
Erythroid	*Kit*	0.0066	0.293	0.059	0.275
T cells	*Kit*	-	-	-	-
Erythroid	*Xpo1*	$2.65x10^{-9}$	0.514	0.0025	0.373
T cells	*Xpo1*	0.238	0.047	0.137	0.066
Erythroid	*Ranbp1*	0.099	0.133	0.41	0.078
T cells	*Ranbp1*	0.278	-0.124	0.970	0.019
Erythroid	*Ranbp2*	$3.2x10^{-14}$	0.755	0.058	0.298
T cells	*Ranbp2*	$4.5x10^{-4}$	0.275	0.210	0.094
Erythroid	*Nr3c1*	$6.5x10^{-4}$	0.319	0.0011	0.447
T cells	*Nr3c1*	0.0018	0.274	0.0018	0.233
Erythroid	*Ddx46*	$1.65x10^{-9}$	0.530	$2.98x10^{-9}$	0.775
T cells	*Ddx46*	$2.3x10^{-5}$	0.348	$7.5x10^{-6}$	0.446
Erythroid	*Hba-a1*	0.906	0.034	0.0088	-2.168

Table 4.

Differential mRNA expression of erythropoietic, stem cell, and proliferation associated markers in reclustered WT, *cd47*$^{-/-}$, and *thbs1*$^{-/-}$ erythroid and T cell clusters.

results in an intrinsic protection of hematopoietic stem cells in bone marrow from genotoxic stress, which may be mediated by an increased protective autophagy response (Soto-Pantoja et al., 2012). The same mechanism may contribute to regulating extramedullary erythropoiesis in spleen.

The properties of erythroid precursors that accumulate in *cd47*$^{-/-}$ spleens are consistent with previous studies of stress induced extramedullary erythropoiesis associated with malaria or trypanosome infections (Delic et al., 2020; Thompson et al., 2010). In addition to containing elevated NK precursors (Nath et al., 2018), the present data demonstrate that *cd47*$^{-/-}$ spleen contains more abundant erythroid precursors that are Ter119^{+} by flow cytometry but presumably lack sufficient Ter119 for antibody bead depletion. These cells are present but less abundant in WT spleen, indicating that a low level of extramedullary erythropoiesis occurs in healthy mouse spleen. The Ter119^{+}CD34^{-} cells that accumulate in *cd47*$^{-/-}$ spleens are more proliferative and express multiple markers of committed erythroid precursors. In contrast, the same cells are depleted in *thbs1*$^{-/-}$ spleen, consistent with the function of thrombospondin-1 to facilitate the CD47/SIRPα-mediated turnover of aging RBC (Wang et al., 2020). These data also indicate that physiological levels of thrombospondin-1 are necessary to support a basal level of erythropoiesis in WT spleen.

Notably, *thbs1*$^{-/-}$ and *cd47*$^{-/-}$ spleens contain more early erythroid precursors than are maintained basally in a WT spleen, consistent with the role of thrombospondin-1 signaling via CD47 to limit the expression of multipotent stem cell transcription factors in spleen (Kaur et al., 2013). Earlier erythroid precursors that are Ter119^{-}Kit^{+} accumulate in *thbs1*$^{-/-}$spleen. *Thbs1*$^{-/-}$ and *cd47*$^{-/-}$ cells express more Ddx46, which is required for differentiation of hematopoietic stem cells (Hirabayashi et al., 2013), and Xpo1, which supports the erythropoietic function of Gata1 (Guillem et al., 2020). Although Ter119^{+} cells expressing markers of committed erythroid progenitors were depleted in *thbs1*$^{-/-}$compared to WT spleens, mRNAs for some markers of committed erythroid cells including Nr3c1 mRNA were elevated in *thbs1*$^{-/-}$ and *cd47*$^{-/-}$cluster 12 cells. However, early progenitors express CD45R, and inclusion of this antibody in the negative selection cocktail should deplete early progenitors from the populations used for both RNAseq analyses. This may account for the relative lack of CD47-dependent CD34^{+} cells in cluster 12.

One caveat in interpreting the CD47- and thrombospondin-1-dependence of the extramedullary erythropoiesis markers Ermap and Aqp1 in total spleen cells and the Ter119-depleted cells used for scRNAseq is that both are also expressed in minor subsets of T cells (Moon et al., 2004). The reclustering analysis confirmed that these erythropoietic markers are expressed in minor T cell populations, which notably also showed CD47-dependent gene expression changes. This may also account for the differences in CD47-dependence of erythropoietic marker expression observed by flow cytometry in Ter119^{+} cells but not in total spleen cells or Ter119^{-} spleen cells.

In addition to utility for assessing extramedullary erythropoiesis, the CD47-dependent erythropoiesis genes identified here may have translational utility. Therapeutic CD47 antibodies and decoys designed to inhibit the function of CD47 have entered multiple clinical trials for treating cancers, but anemia associated with loss of CD47-dependent inhibitory SIRPα signaling in macrophages has been a frequent side effect observed for the first generation of these therapeutics (Kaur et al., 2020). These therapeutic antibodies also recognize CD47 on RBC and thereby sensitize them to removal by phagocytes. The resulting anemia would be expected to induce erythropoiesis in bone marrow and possibly at extramedullary sites. Human spleen cells are not accessible to directly evaluate extramedullary erythropoiesis in cancer patients receiving CD47-targeted therapeutics, but analysis of circulating erythroid precursors or liquid biopsy methods could be useful to detect induction of extramedullary erythropoiesis by these therapeutics. Therefore, the CD47-dependent erythroid markers identified in this study may be useful biomarkers for assessing hematologic side effects of CD47-targeted therapeutics.

Materials and Methods

Key Resources Table				
Reagent type (species) or resource	**Designation**	**Source or reference**	**Identifiers**	**Additional information**
Kit	CD8a+ T Cell Isolation Kit	Miltenyi Biotec	Order no. 130–104-075	
Kit	CD8a (Ly-2) MicroBeads mouse	Miltenyi Biotec	Order no. 130-117-044	
Reagent	EDTA solution	Sigma-Aldrich	E8008	2 mM
Reagent	bovine serum albumin (BSA)	Sigma-Aldrich	A7906	0.5%

Reagent	ACK Lysing Buffer, 100mL	Quality Biologicals	118-156-721	
Mice (M. musculus)	WT, *Cd47*$^{-/-}$ and *Thbs1*$^{-/-}$	Jackson Laboratories	C57BL/6 background	Lindberg et al in 1996; Lawler et al, 1998
Antibodies	APC anti-mouse Ter119	Biolegend	Cat no. 116212 (clone: Ter119)	Rat IgG2b working 1 µg/100 µl/1 million cells
Antibodies	Percp/Cy5.5 anti-mouse CD34	Biolegend	Cat no. 119327 (clone: MEC14.7)	Rat IgG2a working 1 µg/100 µl/1 million cells
Antibodies	PE/Cy7 anti mouse Sca1	Biolegend	Cat no. 108114 (clone: D7)	Rat IgG2a working 0.5 µg/100 µl/1 million cells
Antibodies	PE anti-mouse cKit	Biolegend	Cat no. 105808 (clone: 2B8)	Rat IgG2b working 0.1 µg/100 µl/1 million cells
Antibodies	PE/Cy7 anti-mouse Ki67	Biolegend	Cat no. 652425 (clone: 16A8)	Rat IgG2a working 0.5 µg/100 µl/1 million cells
Antibodies	APC Rat IgG2b, κ Isotype Control Antibody	Biolegend	Cat no. 400611 (clone : RTK4530)	Rat IgG2b working 1 µg/100 µl/1 million cells
Antibodies	PerCP/Cyanine5.5 Rat IgG2a, κ Isotype Control Antibody	Biolegend	Cat no. 400531 (clone : RTK2758)	Rat IgG2a working 1 µg/100 µl/1 million cells

Antibodies	PE/Cyanine7 Rat IgG2a, κ Isotype Control Antibody	Biolegend	Cat no. 400521 (clone : RTK2758)	Rat IgG2a working 0.25 µg/100 µl/1 million cells
Antibodies	PE Rat IgG2b, κ Isotype Control Antibody	Biolegend	Cat no. 400608 (clone : RTK4530)	Rat IgG2b working 0.1 µg/100 µl/1 million cells
Antibodies	Alexa Fluor® 488 Rat IgG2a, κ Isotype Ctrl Antibody	Biolegend	Cat no. 400525 (clone : RTK2758)	Rat IgG2a working 0.25 µg/100 µl/1 million cells
Antibodies	Goat anti-Rabbit IgG (H+L) Cross-Adsorbed Secondary Antibody, Alexa Fluor™ 594	Thermofisher	Cat no. A-11012	Goat anti Rabbit IgG working 0.2 µg/100 µl/1 million cells
Antibodies	ERMAP Polyclonal Antibody	Thermofisher	Cat no. BS-12333R	Rabbit IgG working 1:100 dilution
Antibodies	GYPA Polyclonal Antibody	Thermofisher	Cat no. BS-2575R	Rabbit IgG working 1:100 dilution
Antibodies	Aquaporin 1 Polyclonal Antibody	Thermofisher	Cat no. PA5-78806	Rabbit IgG working 1 µg/100 µl/1 million cells
Antibodies	EPOR Polyclonal Antibody	Bioss; Thermofisher	Cat no. BS-1424R	Rabbit IgG working 1 µg/100 µl/1 million cells

Mice and cells

WT, *cd47*$^{-/-}$ (B6.129S7-Cd47tm1Fpl/J, (Lindberg et al., 1996)), and *thbs1*$^{-/-}$ (B6.129S2-*Thbs1*^{tm1Hyn}/J, (Lawler et al., 1998)) mice were obtained from The Jackson Laboratory, backcrossed on the C57BL/6 background, and maintained under specific pathogen free conditions. All animal experiments were carried out in strict accordance with the Recommendations for the Care and Use of Laboratory Animals of the National Institutes of Health under a protocol approved by the NCI Animal Care and Use Committee. Age and gender matched 8-12 week-old mice were used for experiments except where noted. For the bulk RNA sequencing four male *cd47*$^{-/-}$ mice and four male wildtype mice were used per CCBR guidance. For single cell RNA sequencing two female and one male of each genotype were used per CCBR guidance. For flow cytometry two female and two males of each genotype were used.

Spleens were removed from the mice and homogenized in HBSS and passed through a 70 µm mesh (Sigma, CLS431751) to remove debris. The cell suspension was treated with ACK lysis buffer for 4 minutes to lyse the RBC. The suspensions were centrifuged and washed twice with cold HBSS.

Aliquots of single cell suspensions were stained using trypan blue and counted to assess viability.

Flow cytometry

Spleens were obtained from two male and two female mice of each genotype. Single-cell suspensions from spleens were stained by incubation for 30 min at 4°C using optimized concentrations of antibodies: CD34-Percp/Cy5.5 and Ter119-APC, cKit-PE and PE/Cy7, Sca1-AF488, Ki67-PE-Cy7 and Percp/Cy5.5 (Biolegend). Non-tagged Ermap, Gypa, Aqp1 (Thermofisher) and Epor (Bios Inc.) antibodies were detected using secondary goat anti-rabbit AF594 antibodies. Stained single cell suspensions were acquired on an LSRFortessa SORP (BD Biosciences), and data were analyzed using FlowJo software (Tree Star). A total of 2×10^5 gated live events were acquired for each analysis. Isotype and unstained controls were used to gate the desired positive populations.

Single cell RNA sequencing (scRNAseq)

Because bulk RNA sequencing analysis identified elevated expression of erythropoietic genes in $CD8^+$ spleen cells from *cd47*$^{-/-}$ mice that were obtained using magnetic bead depletion of all other lineages, the same method was used as the first step to enrich erythroid precursors. Single cell suspensions from WT, *thbs1*$^{-/-}$and *cd47*$^{-/-}$ spleens were depleted of all mature hematopoietic cell lineages including erythroblasts and mature RBC using the CD8a+ T Cell Isolation Kit, mouse (Miltenyi Biotec). Single cell suspensions were incubated with the supplied antibody cocktail of the CD8+ T cell isolation kit for 15 min. on ice and then passed through the column as per manufacturer's instructions. The flow through combined with 3 washes was centrifuged, and the cells were then incubated with CD8a (Ly-2) microbeads and passed through magnetic columns to obtain lineage-depleted cell populations. Capture & Library Preparation for single cell end-counting gene expression using the 10X Genomics platform was performed by the Single Cell Analysis Facility (CCR).

Single-cell RNA-sequencing (scRNA-seq) data were generated using the Chromium Single Cell 3' Solution (10x Genomics). Raw sequencing data were processed using the CellRanger software suite (version 4.0.0), 10x Genomics). CellRanger's mkfastq and count functions were utilized to demultiplex raw base call (BCL) files into sample-specific FASTQ files, perform barcode processing, and align cDNA reads to the reference genome (mm10) to generate feature-barcode matrices.

Downstream analysis and visualization were performed within the NIH Integrated Analysis Platform (NIDAP) using R programs developed by a team of NCI bioinformaticians on the Foundry platform (Palantir Technologies). The Single Cell workflow on NIDAP executes the SCWorkflow package (He et al.), which is based on the Seurat workflow (v. 4.1.1) (Hao et al., 2021). Quality control metrics were assessed to remove low-quality cells, defined as cells with fewer than 200 detected genes or a high percentage (>15%) of mitochondrial gene expression, indicative of cellular stress or apoptosis. After filtering, the dataset consisted of 13,933 single cells with an average of 7,523 unique molecular identifiers (UMIs) per cell and an average gene detection of 2,114 genes per cell. The dataset underwent normalization via log-transformation, and RunPCA applied to the scaled data of the variable features to compute the principal components. After performing SCTransform (Hafemeister and Satija, 2019) on the merged dataset, an unsupervised clustering methodology was employed to categorize cells exhibiting analogous expression patterns. The FindClusters function was used with a clustering resolution of 0.4 for all cells and a reclustered resolution of 0.2 for the RBC progenitor cell subset. Each cellular cluster was annotated with the expression of established cell-type-specific marker genes and dimensionality reduction plots (t-distributed stochastic neighbor embedding (t-SNE) and uniform manifold approximation and projection (UMAP)), were utilized for the visual representation of clusters. Cell types were called using SingleR (v.1.0) (Aran et al., 2019) and Immgen and Mouse RNAseq databases.

Differential expression analysis among the identified cell clusters was conducted utilizing the FindMarkers function, which implements a Wilcoxon Rank Sum test. Genes were deemed differentially expressed with an adjusted p-value < 0.05 following correction for multiple testing via the Benjamini-Hochberg procedure.

Bulk RNAseq

Naïve CD8-enriched lineage-depleted spleen cells from four male 4-6 week-old *cd47*$^{-/-}$and four male WT mice were prepared using CD8a+ T Cell Isolation Kit, subjected to RNAseq analysis (Nath et al., 2022). Downstream analysis and visualization were performed within the NIH Integrated Analysis Platform (NIDAP) using R programs developed by a team of NCI bioinformaticians on the Foundry platform (Palantir Technologies). Briefly, RNA-seq FASTQ files were aligned to the reference genome (mm10) using STAR (Dobin et al., 2013) and raw counts data produced using RSEM (Li and Dewey, 2011). The gene counts matrix was imported into the NIDAP platform, where genes were filtered for low counts (<1 cpm) and normalized by quantile normalization using the limma package (Ritchie et al., 2015). Differentially expressed genes were calculated using limma-Voom (Law et al., 2016) and GSEA was performed using the fgsea package (Korotkevich et al., 2019). Preranked gene set enrichment analysis of the Hallmark collection was performed using the t-statistic as ranking variable. (**Figure 1–figure supplement 1**).

Data Sharing Statement

Data supporting this publication have been deposited in NCBI's Gene Expression Omnibus and are accessible through GEO Series accessions GSE239430. Reviewers may access this embargoed data by using the following Reviewer Token: qzuzwawmhpenxel. The code used to produce bioinformatics results can be found at *https://github.com/NIDAP-Community/SCWorkflow* and *https://github.com/NIDAP-Community/Regulation-of-Extramedullary-Erythropoiesis-by-CD47-and-THBS1*. Primary flow cytometry data is available at *https://zenodo.org/records/10904137*. Additional data may be found in Figure supplements available with the online version of this article.

Acknowledgements

We thank Dr. Michael Kelly at the Single Cell Analysis Facility for performing preliminary clustering and data analysis. This research was funded by the Intramural Research Program of the Center for Cancer Research, the National Cancer Institute, and National Institutes of Health (ZIA SC009172, D.D.R.).

Author Contributions

B.: Contribution: Conceptualization, Methodology, Formal analysis, Investigation, Validation, Visualization, Writing – original draft preparation; Writing – review and editing

J. M.: Contribution: Formal analysis, Visualization, Software, Data curation, Writing – review and editing

C. C.: Contribution: Formal analysis, Project administration, Writing – review and editing

K.: Contribution: Conceptualization, Methodology, Formal analysis, Investigation, Writing –original draft preparation; Writing – review and editing

D. R.: Contribution: Conceptualization, Formal analysis, Supervision, Project administration, Funding acquisition, Writing – original draft preparation; Writing – review and editing

Competing interests

No competing interests declared

Figure Supplement Legends

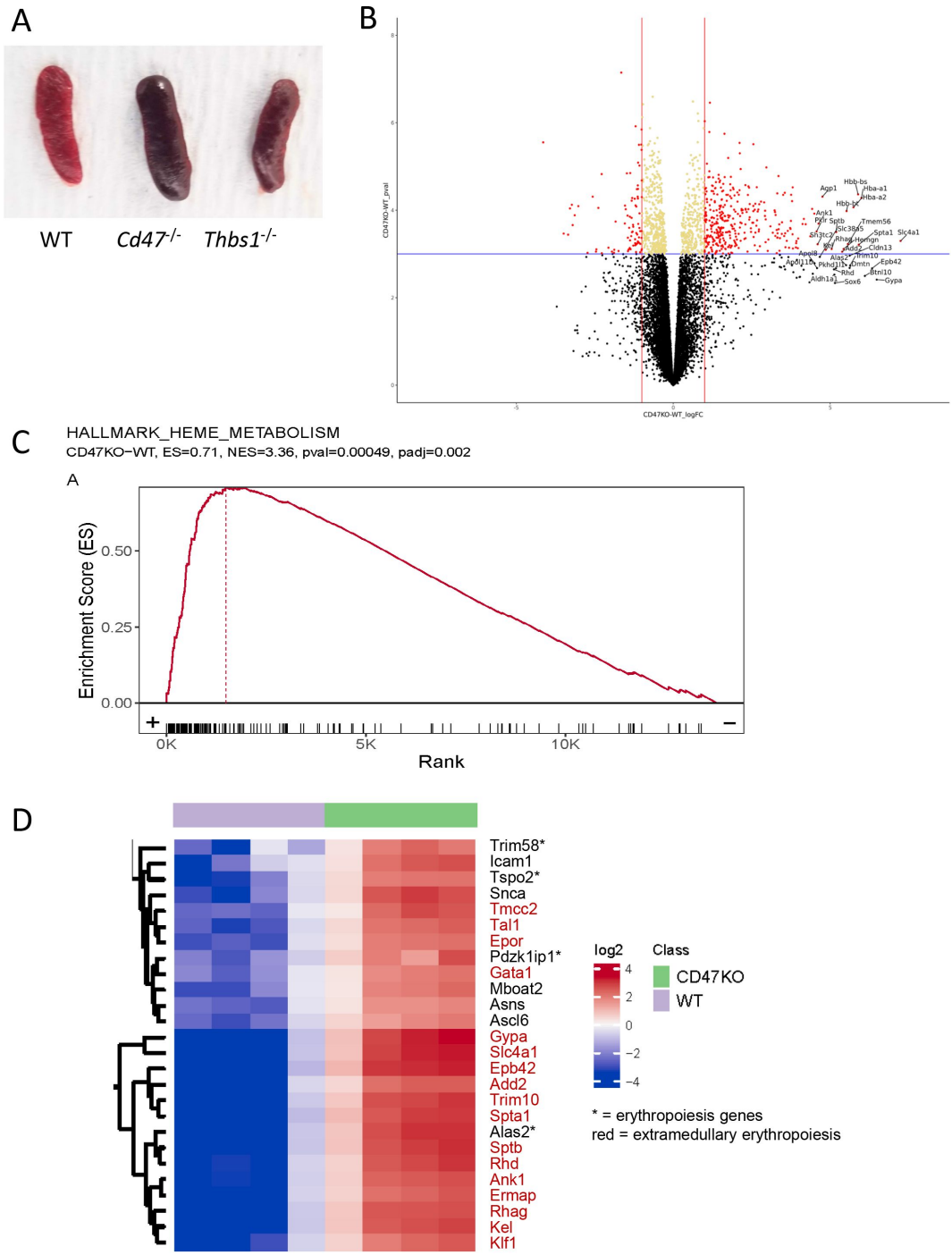

Figure 1–figure supplement 1.

Enlargement of spleen in the absence of CD47 and bulk RNAseq analysis of lin− *cd47*$^{-/-}$ vs WT spleen cells. A) Representative images of spleens from WT, *cd47*$^{-/-}$and *thbs1*$^{-/-}$mice. B) volcano plot for differentially expressed genes between lineage-depleted Naïve *cd47*$^{-/-}$vs WT CD3^{+} spleen cells. Red dots represent significant genes with >2-fold change and p<0.001, and the top 30 genes were labelled. C). GSEA plot showing RBC Heme Metabolism gene set enrichment and, D) Heat map visualization of the top differentially expressed genes in the RBC Heme Metabolism gene set.

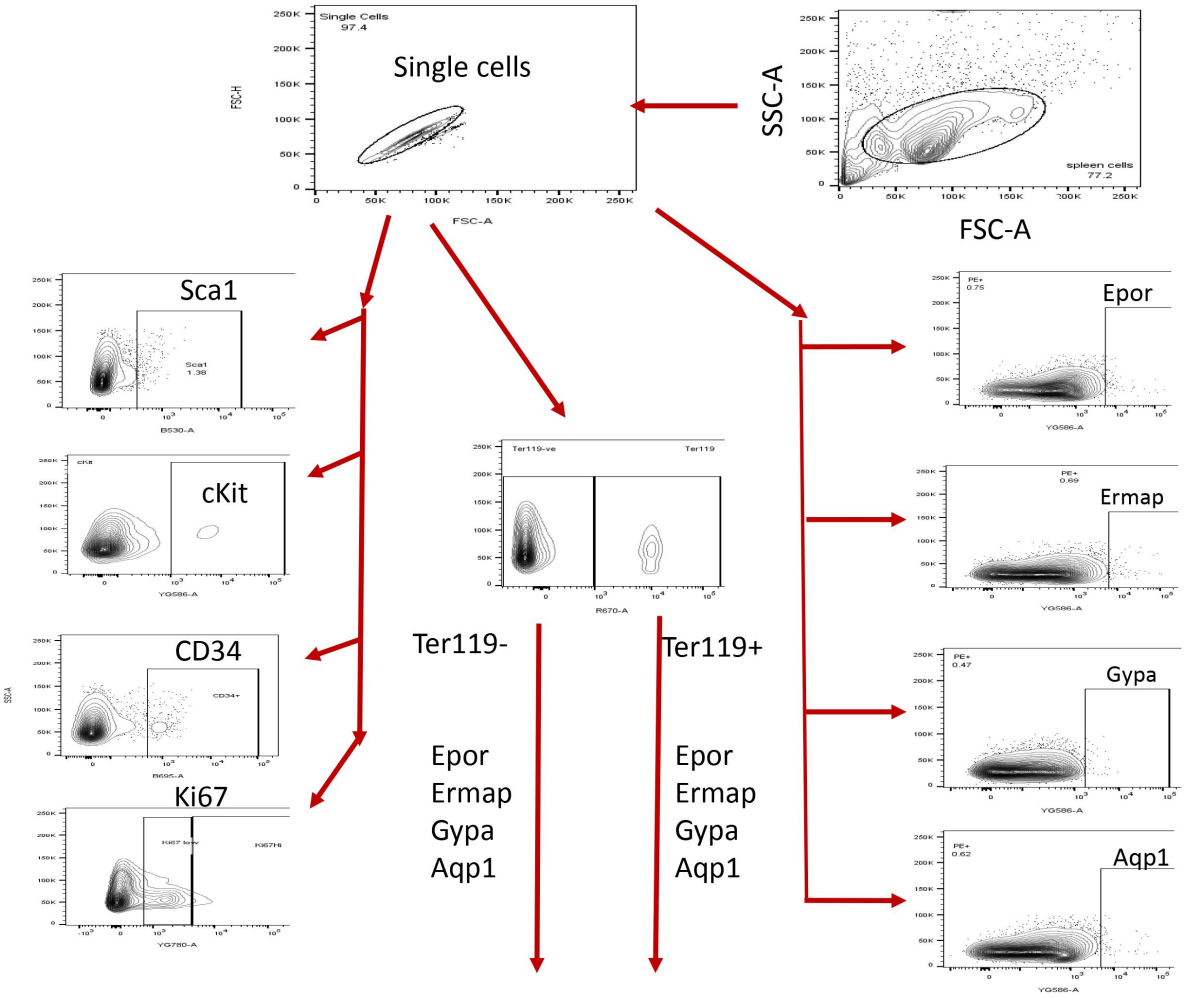

Figure 1–figure supplement 2.

Flow cytometry analysis strategy. The sequential flow cytometry gating strategy is illustrated.

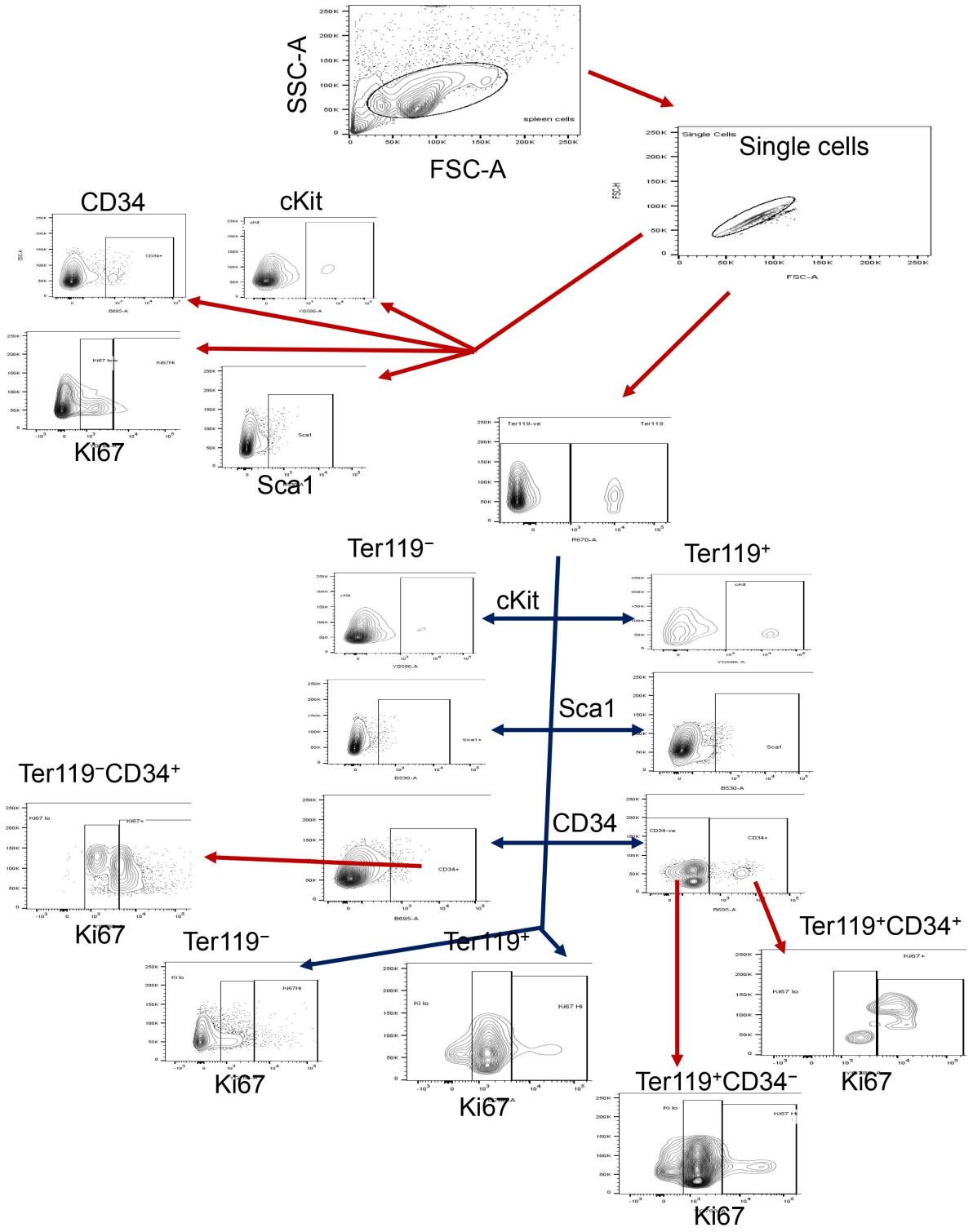

Figure 2–figure supplement 1.

Flow cytometry analysis strategy. The sequential flow cytometry gating strategy is illustrated.

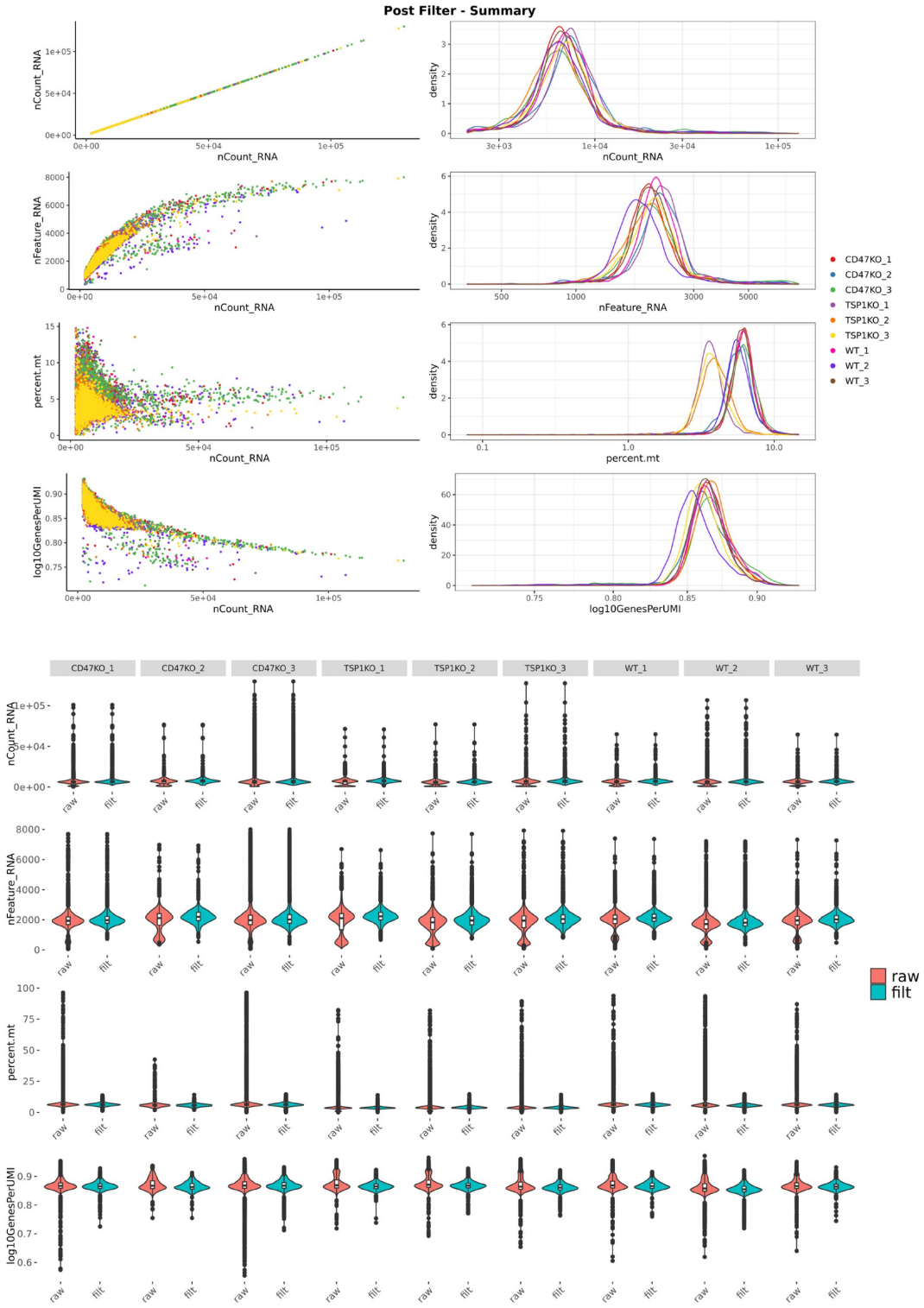

Figure 3–figure supplement.

Single cell RNA sequence post-filter QC plots. The scatter plots, histograms and violin plots of three samples lineage-depleted of WT, *cd47*$^{-/-}$and *thbs1*$^{-/-}$ spleen cells are shown. The number of UMI per cell filter was set to exclude cells with < 2000 UMI in nCount RNA. The Feature RNA plot shows the number of genes with non-zero expression detected per cell. Filtering was set to exclude cells having <15% mitochondrial gene expression as presented in the percent mt plot. The log10Genes per UMI plot represents the scores for complexity of the RNA library found in each cell. No filter was set in this row.

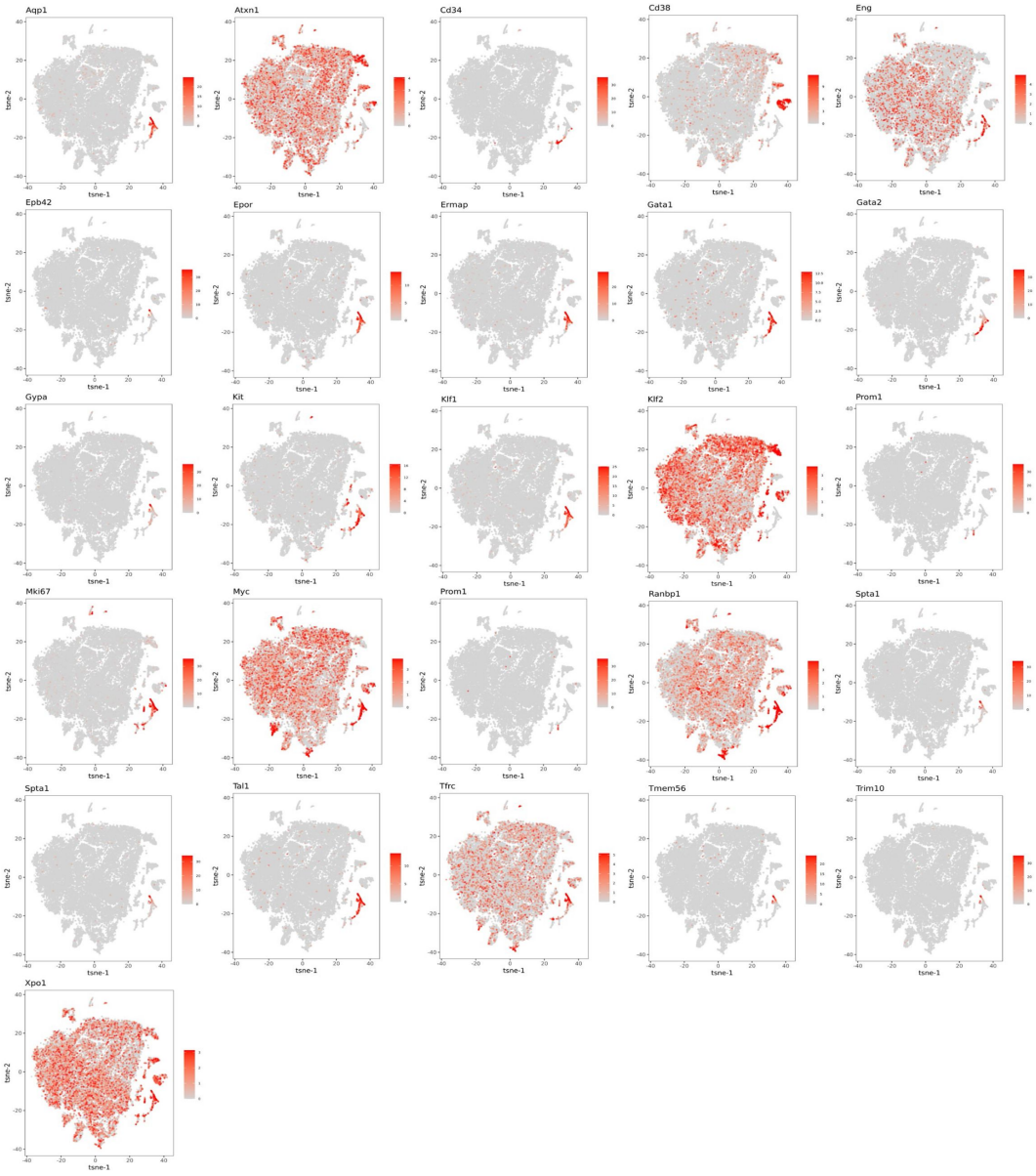

Figure 4–figure supplement 1.

The distributions of mRNA expression of the indicated genes related to stem cells and erythropoietic cells are shown throughout the 18 clusters as a tSNE projection.

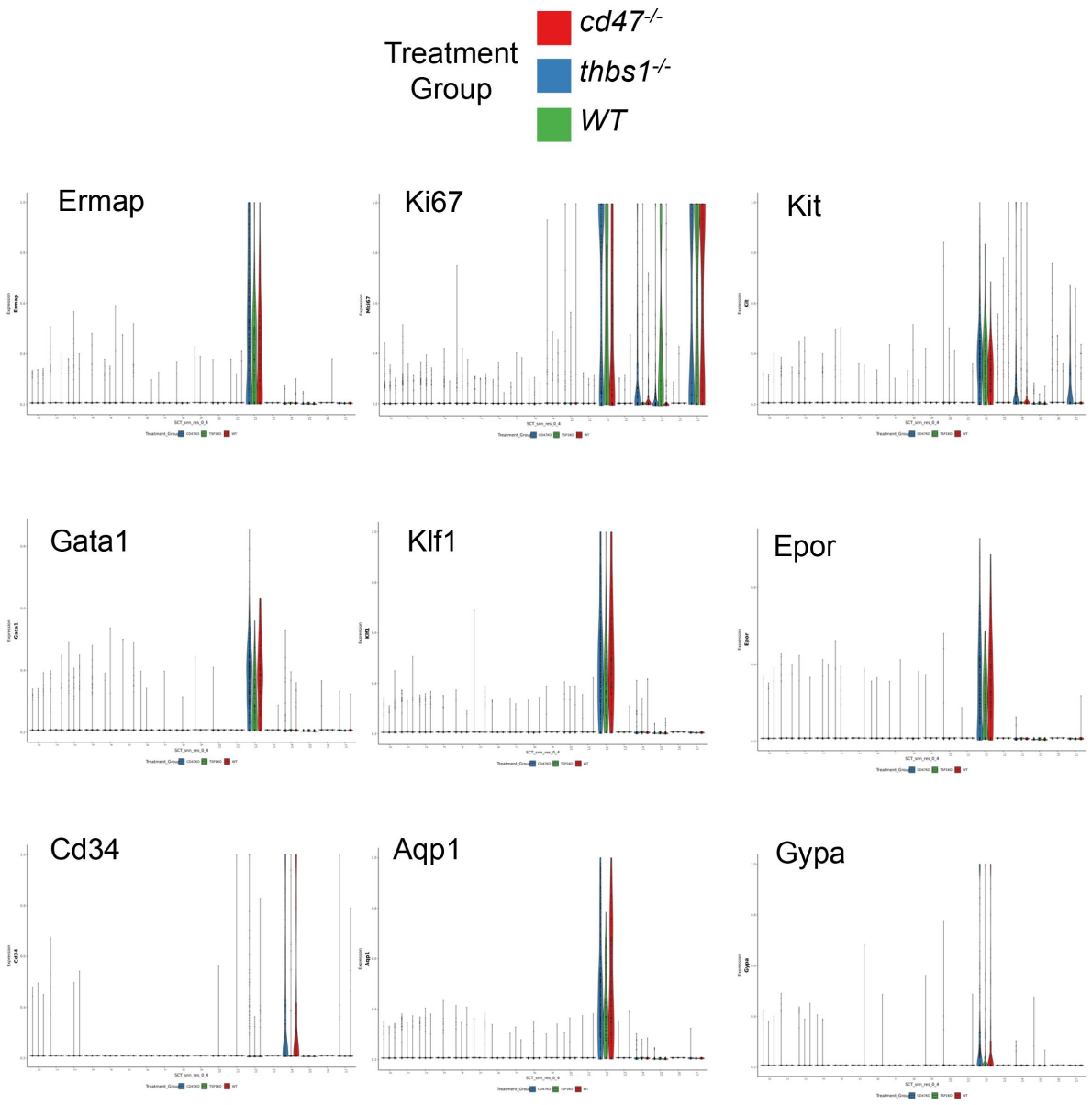

Figure 4–figure supplement 2.

Violin plots of erythropoietic, stem cell, and proliferation associated marker mRNAs expressed in 18 cell clusters.

A

Cluster	Gene	% positive cd47$^{-/-}$ cells	% positive thbs1$^{-/-}$ cells	% positive WT cells
12	Klf1	88.0	79.7	89.1
14	Klf1	-	-	-
12	Aqp1	80.3	78.1	80.4
14	Aqp1	-	-	-
12	Tfrc	44	34.4	35.9
14	Tfrc	13.5	10.7	9.1
12	Epor	58.5	51.6	65.2
12	Ermap	66.9	65.6	64.1
12	Gata1	77.1	53.1	73.9
12	Mki67	74.6	64.1	57.6
14	Mki67	41.1	9.3	24.2
12	Kit	80.6	75.0	67.4
14	Kit	30.7	20.0	13.6
12	Xpo1	67.6	53.1	38.0
14	Xpo1	38.0	30.7	25.8
12	Ranbp1	95.8	98.4	91.3
14	Ranbp1	71.2	54.7	69.7
12	Ranbp2	85.9	64.1	47.8
14	Ranbp2	57.7	38.7	34.8
12	Nr3c1	63.4	68.8	42.4
14	Nr3c1	47.2	64.0	28.8
12	Ddx46	78.9	87.5	50.0
14	Ddx46	50.9	50.7	25.8

B

Cell cluster	mRNA	Cd47$^{-/-}$ vs WT		Thbs1$^{-/-}$ vs WT	
		p-value	Avg FC	p-value	Avg FC
C12	Xpo1	3.3x10^{-8}	1.39	0.0069	1.25
C12 (CD34^{-})	Xpo1	2.3x10^{-8}	1.42	0.010	1.25
C12 (CD34^{+})	Xpo1	NS		-*	
C14	Xpo1	NS		NS	
C12	Ranbp2	4.3x10^{-14}	1.69	NS	
C12 (CD34^{-})	Ranbp2	3.8x10^{-15}	1.76	NS	
C12 (CD34^{+})	Ranbp2	NS		-*	
C14	Ranbp2	0.0055	1.29	NS	

*Insufficient CD34^{+} *thbs1*$^{-/-}$ cells to calculate

C

Gene	P-val *Cd47*$^{-/-}$ vs WT	Avg log2FC *Cd47*$^{-/-}$ vs_WT	P-val *Thbs1-/-* vs_WT	Avg log2FC *Thbs1-/-* vs_WT
mt-Atp6	0.887	-0.027	5.43x10^{-11}	-0.812
mt-Atp8	7.23x10^{-20}	0.98	0.0168	0.377
mt-Co1	0.028	0.135	2.60x10^{-7}	-0.532
mt-Co2	0.226	0.068	3.37x10^{-10}	-0.693
mt-Co3	0.207	0.097	1.02x10^{-8}	-0.671
mt-Cytb	0.338	-0.006	9.35x10^{-10}	-0.790
mt-Nd1	0.074	0.15	6.78x10^{-6}	-0.636
mt-Nd2	0.135	0.113	1.00x10^{-7}	-0.748
mt-Nd3	7.67x10^{-9}	0.531	1.36x10^{-7}	-0.813
mt-Nd4	0.152	0.093	5.84x10^{-6}	-0.558
mt-Nd4l	3.50x10^{-10}	0.658	6.49x10^{-8}	0.787
mt-Nd5	4.63x10^{-8}	0.612	0.0154	0.375
mt-Nd6	1.65x10^{-7}	0.416	4.39x10^{-6}	0.524

Figure 4–figure supplement 3.

Differential expression of erythropoietic, stem cell, and proliferation associated markers in cell clusters 12 and 14. (A) Percentages of cells with detectable mRNA expression of the indicated erythropoietic, stem and proliferative markers in cluster 12 and cluster 14 in WT, cd47$^{-/-}$, and *thbs1*$^{-/-}$ spleens. (B) Differential mRNA expression of the nuclear export protein Xpo1 and nuclear pore protein synthesis instructor Ranbp2, which increase erythropoiesis by stabilizing Gata1 in the nucleus, in cluster12 and CD34+ and CD34− subsets of cluster 12 cells. (C) Differential expression of mitochondrial-encoded genes in cluster 12 cells from WT, cd47$^{-/-}$, and *thbs1*$^{-/-}$ spleens.

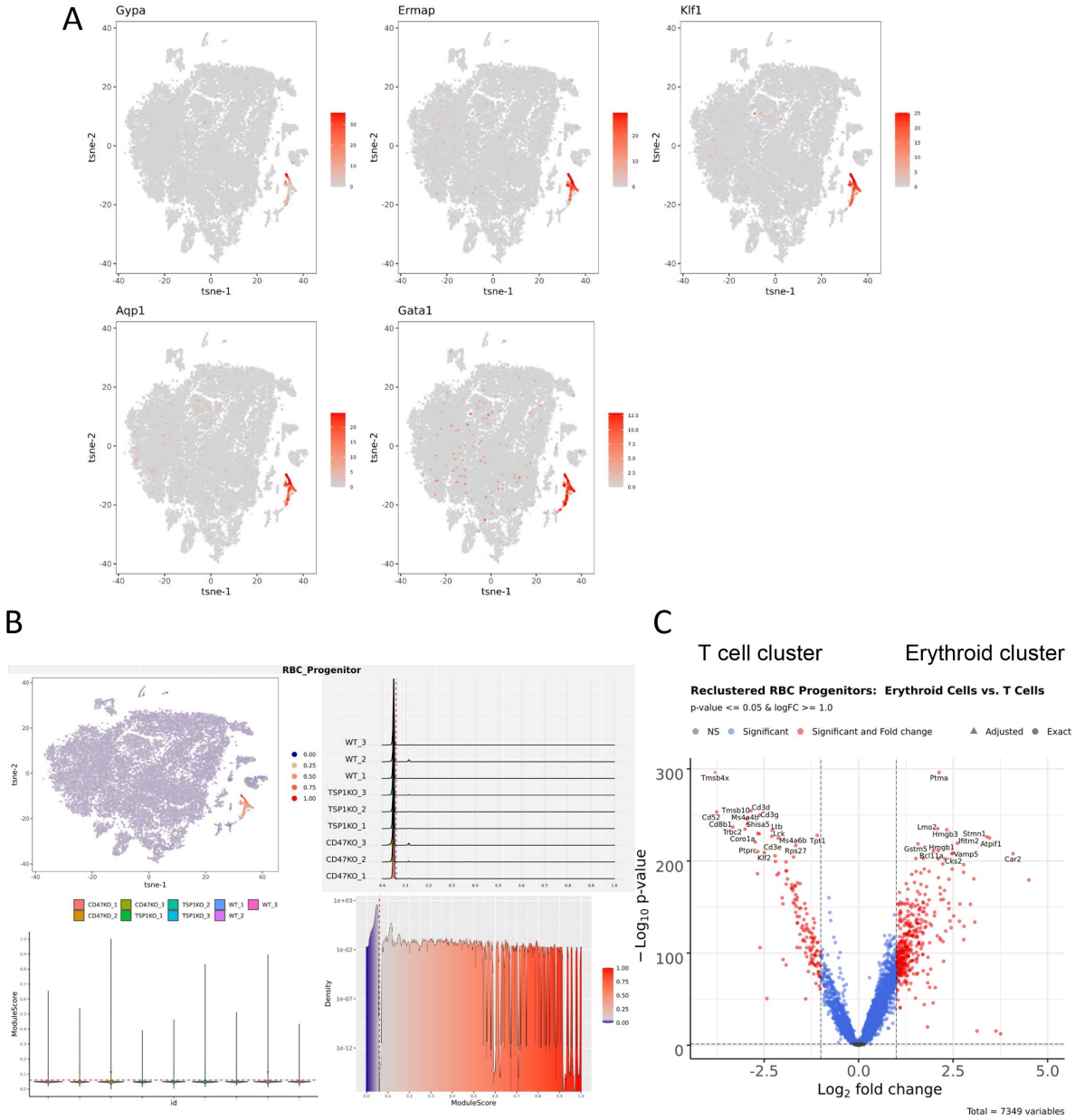

Figure 6–figure supplement 1.

Strategy for reclustering spleen cells that express a gene signature for committed erythroid precursors. (A) The left panels show the distribution of cells expressing threshold levels of the 5 gene signature in the original TSNE projection. (B) The RBC progenitor module scoring was performed, as module Scores (a.k.a. Signature Scores) calculated for each cell using expression of five genes (Gypa, Ermap, Klf1, Gata1, and Aqp1). The threshold was set manually (red dashed line on subplots) to separate high-scoring cells from low-scoring cells and expressed by the color on the TSNE plot (top left, high score cells are dark red and low scores cells are represented as light red). RBC Progenitor Module Scoring Plots show the distributions of module scores in lineage-depleted spleen cells from each mouse, with the threshold score indicated by the dotted red lines. (C) The volcano plot presents differentially expressed genes contrasting the reclustered erythropoietic progenitor cell clusters and the T cell cluster.

Cluster	Gene	% positive cd47$^{-/-}$ cells	% positive thbs1$^{-/-}$ cells	% positive WT cells
Erythroid	Klf1	91.5	84.5	99.1
T cells	Klf1	25.6	21.4	26.0
Erythroid	Aqp1	78.9	83.0	84.5
T cells	Aqp1	32.2	21.4	28.9
Erythroid	Tfrc	45.8	37.9	36.7
T cells	Tfrc	-	-	-
Erythroid	Epor	60.1	56.9	64.4
Erythroid	Ermap	70.7	65.6	64.4
T cells	Ermap	26.4	23.9	20.2
Erythroid	Gata1	80.8	58.6	75.6
Erythroid	Mki67	77.1	69.0	58.9
T cells	Mki67	-	-	-
Erythroid	Kit	80.1	77.6	68.9
T cells	Kit	-	-	-
Erythroid	Xpo1	69.4	56.9	37.8
T cells	Xpo1	21.7	23.9	16.8
Erythroid	Ranbp1	96.7	98.4	91.1
T cells	Ranbp1	54.3	61.5	60.1
Erythroid	Ranbp2	86.7	67.2	48.9
T cells	Ranbp2	46.1	36.8	27.7
Erythroid	Nr3c1	63.5	67.2	41.1
T cells	Nr3c1	44.2	47.9	27.7
Erythroid	Ddx46	81.5	86.2	50.0
T cells	Ddx46	55.0	59.8	33.5
Erythroid	Hba-a1	23.6	6.9	25.6
T cells	Hba-a1	-	-	-

Figure 7–figure supplement 1.

Differential expression of erythropoietic, stem cell, and proliferation associated markers in reclustered erythroid and T cell clusters. The percent of cells positive for expression of the indicated genes in WT, cd47$^{-/-}$, and *thbs1*$^{-/-}$ cells is presented in the indicated clusters. (-) indicates no cells in the cluster expressed detectable levels of the indicated gene.

References

Aran D. *et al.* (2019) **Reference-based analysis of lung single-cell sequencing reveals a transitional profibrotic macrophage** *Nature immunology* **20**:163–172 https://doi.org/10.1038/s41590-018-0276-y

Bian Z. *et al.* (2016) **Cd47-Sirpalpha interaction and IL-10 constrain inflammation-induced macrophage phagocytosis of healthy self-cells** *Proceedings of the National Academy of Sciences of the United States of America* **113**:E5434–5443 https://doi.org/10.1073/pnas.1521069113

Burger P., Hilarius-Stokman P., de Korte D., van den Berg T.K., van Bruggen R. (2012) **CD47 functions as a molecular switch for erythrocyte phagocytosis** *Blood* **119**:5512–5521 https://doi.org/10.1182/blood-2011-10-386805

Cenariu D., Iluta S., Zimta A.A., Petrushev B., Qian L., Dirzu N., Tomuleasa C., Bumbea H., Zaharie F. (2021) **Extramedullary Hematopoiesis of the Liver and Spleen** *J Clin Med* **10** https://doi.org/10.3390/jcm10245831

Delic D., Wunderlich F., Al-Quraishy S., Abdel-Baki A.S., Dkhil M.A., Arauzo-Bravo M.J. (2020) **Vaccination accelerates hepatic erythroblastosis induced by blood-stage malaria** *Malar J* **19** https://doi.org/10.1186/s12936-020-3130-2

Dobin A., Davis C.A., Schlesinger F., Drenkow J., Zaleski C., Jha S., Batut P., Chaisson M., Gingeras T.R. (2013) **STAR: ultrafast universal RNA-seq aligner** *Bioinformatics* **29**:15–21 https://doi.org/10.1093/bioinformatics/bts635

Fossati-Jimack L., Azeredo da Silveira S., Moll T., Kina T., Kuypers F.A., Oldenborg P.A., Reininger L., Izui S. (2002) **Selective increase of autoimmune epitope expression on aged erythrocytes in mice: implications in anti-erythrocyte autoimmune responses** *J Autoimmun* **18**:17–25 https://doi.org/10.1006/jaut.2001.0563

Frazier E., Isenberg J., Shiva S., Zhao L., Schlesinger P., Dimitry J., Abu-Asab M., Tsokos M., Roberts D., Frazier W. (2011) **Age-dependent regulation of skeletal muscle mitochondria by the thrombospondin-1 receptor CD47** *Matrix Biology* **30**:154–161 https://doi.org/10.1016/j.matbio.2010.12.004

Gao A.-G., Lindberg F.P., Finn M.B., Blystone S.D., Brown E.J., Frazier W.A. (1996) **Integrin-associated protein is a receptor for the C-terminal domain of thrombospondin** *The Journal of biological chemistry* **271**:21–24

Guillem F. *et al.* (2020) **XPO1 regulates erythroid differentiation and is a new target for the treatment of beta-thalassemia** *Haematologica* **105**:2240–2249 https://doi.org/10.3324/haematol.2018.210054

Gutierrez L., Caballero N., Fernandez-Calleja L., Karkoulia E., Strouboulis J. (2020) **Regulation of GATA1 levels in erythropoiesis** *IUBMB Life* **72**:89–105 https://doi.org/10.1002/iub.2192

Hafemeister C., Satija R. (2019) **Normalization and variance stabilization of single-cell RNA-seq data using regularized negative binomial regression** *Genome Biol* **20** https://doi.org/10.1186/s13059-019-1874-1

Hao Y. *et al.* (2021) **Integrated analysis of multimodal single-cell data** *Cell* **184**:3573–3587 https://doi.org/10.1016/j.cell.2021.04.048

Harada H., Harada Y., O'Brien D.P., Rice D.S., Naeve C.W., Downing J.R. (1999) **HERF1, a novel hematopoiesis-specific RING finger protein, is required for terminal differentiation of erythroid cells** *Molecular and cellular biology* **19**:3808–3815 https://doi.org/10.1128/MCB.19.5.3808

He R., Cam M., lovbanovav A.M., Michalowski T.J., Meyer G., Zaki **NIDAP Community/SCWorkflow Package**

Hirabayashi R., Hozumi S., Higashijima S., Kikuchi Y. (2013) **Ddx46 is required for multi-lineage differentiation of hematopoietic stem cells in zebrafish** *Stem Cells Dev* **22**:2532–2542 https://doi.org/10.1089/scd.2012.0623

Isenberg J.S., Annis D.S., Pendrak M.L., Ptaszynska M., Frazier W.A., Mosher D.F., Roberts D.D. (2009) **Differential interactions of thrombospondin-1, -2, and -4 with CD47 and effects on cGMP signaling and ischemic injury responses** *The Journal of biological chemistry* **284**:1116–1125 https://doi.org/10.1074/jbc.M804860200

Kaur S., Cicalese K.V., Bannerjee R., Roberts D.D. (2020) **Preclinical and Clinical Development of Therapeutic Antibodies Targeting Functions of CD47 in the Tumor Microenvironment** *Antib Ther* **3**:179–192 https://doi.org/10.1093/abt/tbaa017

Kaur S. *et al.* (2022) **CD47 interactions with exportin-1 limit the targeting of m(7)G-modified RNAs to extracellular vesicles** *Journal of cell communication and signaling* **16**:397–419 https://doi.org/10.1007/s12079-021-00646-y

Kaur S. *et al.* (2013) **Thrombospondin-1 Signaling through CD47 Inhibits Self-renewal by Regulating c-Myc and Other Stem Cell Transcription Factors** *Scientific reports* **3** https://doi.org/10.1038/srep01673

Kelm N.Q., Beare J.E., Weber G.J., LeBlanc A.J. (2020) **Thrombospondin-1 mediates Drp-1 signaling following ischemia reperfusion in the aging heart** *FASEB Bioadv* **2**:304–314 https://doi.org/10.1096/fba.2019-00090

Kidder K., Bian Z., Shi L., Liu Y. (2020) **Inflammation Unrestrained by SIRPalpha Induces Secondary Hemophagocytic Lymphohistiocytosis Independent of IFN-gamma** *J Immunol* **205**:2821–2833 https://doi.org/10.4049/jimmunol.2000652

Kim C.H (2010) **Homeostatic and pathogenic extramedullary hematopoiesis** *J Blood Med* **1**:13–19 https://doi.org/10.2147/JBM.S7224

Kim J.I., Park J.S., Kwak J., Lim H.J., Ryu S.K., Kwon E., Han K.M., Nam K.T., Lee H.W., Kang B.C. (2018) **CRISPR/Cas9-mediated knockout of CD47 causes hemolytic anemia with splenomegaly in C57BL/6 mice** *Lab Anim Res* **34**:302–310 https://doi.org/10.5625/lar.2018.34.4.302

Kina T., Ikuta K., Takayama E., Wada K., Majumdar A.S., Weissman I.L., Katsura Y. (2000) **The monoclonal antibody TER-119 recognizes a molecule associated with glycophorin A and specifically marks the late stages of murine erythroid lineage** *British journal of haematology* **109**:280–287 https://doi.org/10.1046/j.1365-2141.2000.02037.x

Kingsley P.D., Greenfest-Allen E., Frame J.M., Bushnell T.P., Malik J., McGrath K.E., Stoeckert C.J., Palis J. (2013) **Ontogeny of erythroid gene expression** *Blood* **121**:e5–e13 https://doi.org/10.1182/blood-2012-04-422394

Korotkevich G., Sukhov V., Sergushichev A. (2019) **Fast Gene Set Enrichment Analysis** *bioRxiv* https://doi.org/10.1101/060012

Law C.W., Alhamdoosh M., Su S., Dong X., Tian L., Smyth G.K., Ritchie M.E. (2016) **RNA-seq analysis is easy as 1-2-3 with limma, Glimma and edgeR** . *F1000Res* **5** https://doi.org/10.12688/f1000research.9005.3

Lawler J., Sunday M., Thibert V., Duquette M., George E.L., Rayburn H., Hynes R.O. (1998) **Thrombospondin-1 is required for normal murine pulmonary homeostasis and its absence causes pneumonia** *The Journal of clinical investigation* **101**:982–992

Lennartsson J., Ronnstrand L. (2012) **Stem cell factor receptor/c-Kit: from basic science to clinical implications** *Physiological reviews* **92**:1619–1649 https://doi.org/10.1152/physrev.00046.2011

Li B., Dewey C.N. (2011) **RSEM: accurate transcript quantification from RNA-Seq data with or without a reference genome** *BMC Bioinformatics* **12** https://doi.org/10.1186/1471-2105-12-323

Lindberg F.P., Bullard D.C., Caver T.E., Gresham H.D., Beaudet A.L., Brown E.J. (1996) **Decreased resistance to bacterial infection and granulocyte defects in IAP-deficient mice** *Science* **274**:795–798

Lutz H.U., Bogdanova A. (2013) **Mechanisms tagging senescent red blood cells for clearance in healthy humans** *Frontiers in physiology* **4** https://doi.org/10.3389/fphys.2013.00387

Mahajan V.S., Alsufyani F., Mattoo H., Rosenberg I., Pillai S. (2019) **Alterations in sialic-acid O-acetylation glycoforms during murine erythrocyte development** *Glycobiology* **29**:222–228 https://doi.org/10.1093/glycob/cwy110

Matozaki T., Murata Y., Okazawa H., Ohnishi H. (2009) **Functions and molecular mechanisms of the CD47-SIRPalpha signalling pathway** *Trends Cell Biol* **19**:72–80 https://doi.org/10.1016/j.tcb.2008.12.001

Maxhimer J.B., Soto-Pantoja D.R., Ridnour L.A., Shih H.B., DeGraff W.G., Tsokos M., Wink D.A., Isenberg J.S., Roberts D.D. (2009) **Radioprotection in normal tissue and delayed tumor growth by blockade of CD47 signaling** *Sci. Transl. Med* **1** https://doi.org/10.1126/scitranslmed.3000139

Miller T.W., Soto-Pantoja D.R., Schwartz A.L., Sipes J.M., DeGraff W.G., Ridnour L.A., Wink D.A., Roberts D.D. (2015) **CD47 globally regulates metabolic pathways that control resistance to ionizing radiation** *The Journal of biological chemistry* **290**:24858–24874 https://doi.org/10.1074/jbc.M115.665752

Moon C., Rousseau R., Soria J.C., Hoque M.O., Lee J., Jang S.J., Trink B., Sidransky D., Mao L. (2004) **Aquaporin expression in human lymphocytes and dendritic cells** *American journal of hematology* **75**:128–133 https://doi.org/10.1002/ajh.10476

Nath P.R., Gangaplara A., Pal-Nath D., Mandal A., Maric D., Sipes J.M., Cam M., Shevach E.M., Roberts D.D. (2018) **CD47 expression in natural killer cells regulates homeostasis and modulates immune response to lymphocytic choriomeningitis virus** *Frontiers in immunology* **9** https://doi.org/10.3389/fimmu.2018.02985

Nath P.R., Pal-Nath D., Kaur S., Gangaplara A., Meyer T.J., Cam M.C., Roberts D.D. (2022) **Loss of CD47 alters CD8+ T cell activation in vitro and immunodynamics in mice** *Oncoimmunology* **11** https://doi.org/10.1080/2162402X.2022.2111909

Norman-Burgdolf H., Li D., Sullivan P., Wang S. (2020) **CD47 differentially regulates white and brown fat function** *Biol Open* **9** https://doi.org/10.1242/bio.056747

Oldenborg P.A., Zheleznyak A., Fang Y.F., Lagenaur C.F., Gresham H.D., Lindberg F.P. (2000) **Role of CD47 as a marker of self on red blood cells** *Science* **288**:2051–2054 https://doi.org/10.1126/science.288.5473.2051

Perreault A.A., Venters B.J. (2018) **Integrative view on how erythropoietin signaling controls transcription patterns in erythroid cells** *Curr Opin Hematol* **25**:189–195 https://doi.org/10.1097/MOH.0000000000000415

Porpiglia E. *et al.* (2022) **Elevated CD47 is a hallmark of dysfunctional aged muscle stem cells that can be targeted to augment regeneration** *Cell Stem Cell* **29**:1653–1668 https://doi.org/10.1016/j.stem.2022.10.009

Ritchie M.E., Phipson B., Wu D., Hu Y., Law C.W., Shi W., Smyth G.K. (2015) **. limma powers differential expression analyses for RNA-sequencing and microarray studies** *Nucleic acids research* **43** https://doi.org/10.1093/nar/gkv007

Ritterhoff T., Das H., Hofhaus G., Schroder R.R., Flotho A., Melchior F. (2016) **The RanBP2/RanGAP1*SUMO1/Ubc9 SUMO E3 ligase is a disassembly machine for Crm1-dependent nuclear export complexes** *Nature communications* **7** https://doi.org/10.1038/ncomms11482

Soto-Pantoja D.R., Kaur S., Roberts D.D. (2015) **CD47 signaling pathways controlling cellular differentiation and responses to stress** *Critical reviews in biochemistry and molecular biology* **50**:212–230 https://doi.org/10.3109/10409238.2015.1014024

Soto-Pantoja D.R., Miller T.W., Pendrak M.L., Degraff W.G., Sullivan C., Ridnour L.A., Abu-Asab M., Wink D.A., Tsokos M., Roberts D.D. (2012) **CD47 deficiency confers cell and tissue radioprotection by activation of autophagy** *Autophagy* **8**:1628–1642 https://doi.org/10.4161/auto.21562

Strowig T., Rongvaux A., Rathinam C., Takizawa H., Borsotti C., Philbrick W., Eynon E.E., Manz M.G., Flavell R.A. (2011) **Transgenic expression of human signal regulatory protein alpha in Rag2-/-gamma(c)-/-mice improves engraftment of human hematopoietic cells in humanized mice** *Proceedings of the National Academy of Sciences of the United States of America* **108**:13218–13223 https://doi.org/10.1073/pnas.1109769108

Su M., Lin Y., Cui C., Tian X., Lai L. (2021) **ERMAP is a B7 family-related molecule that negatively regulates T cell and macrophage responses** *Cellular & molecular immunology* **18**:1920–1933 https://doi.org/10.1038/s41423-020-0494-8

Swaminathan A., Hwang Y., Winward A., Socolovsky M. (2022) **Identification and Isolation of Burst-Forming Unit and Colony-Forming Unit Erythroid Progenitors from Mouse Tissue by Flow Cytometry** *J Vis Exp* https://doi.org/10.3791/64373

Teruya S., Okamura T., Komai T., Inoue M., Iwasaki Y., Sumitomo S., Shoda H., Yamamoto K., Fujio K. (2018) **Egr2-independent, Klf1-mediated induction of PD-L1 in CD4(+) T cells** *Scientific reports* **8** https://doi.org/10.1038/s41598-018-25302-1

Thompson P.D., Tipney H., Brass A., Noyes H., Kemp S., Naessens J., Tassabehji M. (2010) **Claudin 13, a member of the claudin family regulated in mouse stress induced erythropoiesis** *PloS one* **5** https://doi.org/10.1371/journal.pone.0012667

Wang F., Liu Y.H., Zhang T., Gao J., Xu Y., Xie G.Y., Zhao W.J., Wang H., Yang Y.G. (2020) **Aging-associated changes in CD47 arrangement and interaction with thrombospondin-1 on red blood cells visualized by super-resolution imaging** *Aging Cell* **19** https://doi.org/10.1111/acel.13224

Wang H., VerHalen J., Madariaga M.L., Xiang S., Wang S., Lan P., Oldenborg P.A., Sykes M., Yang Y.G. (2007) **Attenuation of phagocytosis of xenogeneic cells by manipulating CD47** *Blood* **109**:836–842 https://doi.org/10.1182/blood-2006-04-019794

Yang C., Yokomori R., Chua L.H., Tan S.H., Tan D.Q., Miharada K., Sanda T., Suda T. (2022) **Mitochondria transfer mediates stress erythropoiesis by altering the bioenergetic profiles of early erythroblasts through CD47** *The Journal of experimental medicine* **219** https://doi.org/10.1084/jem.20220685

Editors

Reviewing Editor
Jiwon Shim
Hanyang University, Seoul, Korea, the Republic of

Senior Editor
Utpal Banerjee
University of California, Los Angeles, Los Angeles, United States of America

Reviewer #1 (Public Review):

Summary:

This study investigated the role of CD47 and TSP1 in extramedullary erythropoiesis by utilization of both global CD47-/- mice and TSP1-/- mice.

Strengths:

Flow cytometry combined with spleen bulk and single cell transcriptomics were employed. The authors found that stress-induced erythropoiesis markers were increased in CD47-/- spleen cells, particularly genes that are required for terminal erythroid differentiation. Moreover, CD47 dependent erythroid precursors population was identified by spleen scRNA sequencing. In contrast, the same cells were not detected in TSP1-/- spleen. These findings provide strong evidence to support the conclusion that differential role of CD47 and TSP1 in extramedullary erythropoiesis in mouse spleen. Furthermore, the relevance of the current finding to the prevalent side effect (anemia) of anti-CD47 mediated cancer therapy has been discussed in the Discussion section.

https://doi.org/10.7554/eLife.92679.2.sa1

Reviewer #3 (Public Review):

The authors used existing mouse models to compare the effects of ablating the CD47 receptor and its signaling ligand Thrombospondin. They analyze the cell composition of the spleens from CD47-KO and Thsp-KO using Flow Cytometry and single cell sequencing and focus mostly on early hematopoietic and erythroid populations. The data broadly shows that splenomegaly in the CD47-KO is largely due to an increase in committed erythroid progenitors, whereas the Thsp-KO shows a slight depletion of committed erythroid progenitors but is otherwise similar to WT in splenic cell composition. Thus, both their datasets supports the main conclusions of the study. One caveat of the single-cell dataset is that, insofar as the authors have explored and presented it, a clear picture of the mechanism driving extra medullary erythropoiesis in CD47-KO is lacking. This would be extremely valuable since one of the stated translational implications of this study is to assess and remedy the anemia caused by anti-CD47 therapy used in subtypes of AML. Nevertheless, this study provides novel insights into a putative role of Thsp-CD47 signaling in triggering definitive erythropoiesis in the mouse spleen in response to anemic stress and constitutes a good resource for researchers seeking to understand extramedullary erythropoiesis. This study also has generated data that will enable exploration of the possible adverse effects of using anti-CD47 therapies to treat AML.

https://doi.org/10.7554/eLife.92679.2.sa0

Author response:

The following is the authors' response to the original reviews.

Public Reviews:

Reviewer #1 (Public Review):

> *Summary:*
>
> *This study investigated the role of CD47 and TSP1 in extramedullary erythropoiesis by utilization of both global CD47-/- mice and TSP1-/- mice.*
>
> *Strengths:*
>
> *Flow cytometry combined with spleen bulk and single-cell transcriptomics were employed. The authors found that stress-induced erythropoiesis markers were increased in CD47-/- spleen cells, particularly genes that are required for terminal erythroid differentiation. Moreover, CD47 dependent erythroid precursors population was identified by spleen scRNA sequencing. In contrast, the same cells were not detected in TSP1-/- spleen. These findings provide strong evidence to support the conclusion that the differential role of CD47 and TSP1 in extramedullary erythropoiesis in mouse spleen.*
>
> *Weaknesses:*
>
> *Methods and data analysis are appropriate. However, some clarifications are required. The discussion section needs to be expanded.*
>
> *(1) The sex of mice that were used in the study is unknown.*

> *(2) In the method of Single-cell RNA sequencing (page 10), it mentioned that single cell suspensions from mouse spleens were depleted of all mature hematopoietic cell lineages by passing through CD8a microbeads and CD8a+ T cell isolation Kit. As described, it is confusing what cell types are obtained for performing scRNAseq. More information is required for clarity.*
>
> *(3) The constitutive CD47 knockout mouse model is utilized in this study. The observed accumulation of erythroid precursors in the spleens of CD47-/- mice suggests a chronic effect of CD47 on spleen function. Can the current findings be extrapolated to acute scenarios involving CD47 knockdown or loss, as this may have more direct relevance to the potential side effects associated with an-CD47-mediated cancer therapy? Please expand on this topic in the discussion section.*

(1) The missing mouse gender information is incorporated into the revised manuscript. For flow cytometry, two male and two female mice of each genotype were used. For single cell RNA sequencing, two female and one male mouse of each genotype were used. For the bulk RNA sequencing four male *cd47−/−* mice and four male wildtype mice were used.

(2) We apologize for the confusing presentation, which has been corrected. The bulk RNA sequencing analysis identified elevated expression of erythropoietic genes in CD8+ spleen cells from *cd47−/−* versus wildtype mice that were obtained using magnetic bead depletion of all other lineages. Therefore, we used the same Miltenyi negative selection kit as the first step to prepare the cells for single cell RNA sequencing. These untouched cells were then depleted of most mature CD8 T cells using a Miltenyi CD8a(Ly2) antibody positive selection kit. An important consideration underlying this approach was recognizing that the commercial magnetic bead depletion kits used for preparing specific immune cell types are optimized to give relatively pure populations of the intended immune cells using wildtype mice. Our previous experience studying NK cell development in the *cd47−/−* mice taught us that NK precursors, which are rare in wildtype mouse spleens, accumulate in *cd47−/−* spleens and were not removed by the antibody cocktail optimized for wildtype spleen cells (Nath et al Front Immunol 2018). The present data indicate that erythroid precursors behave similarly.

(3) The Discussion was edited as recommended. Anemia is a prevalent side effect of several CD47 therapeutic antibodies being developed for cancer therapy. This anemia would be expected to induce erythropoiesis in bone marrow and possibly at extramedullary sites. Human spleen cells are not accessible to directly evaluate extramedullary erythropoiesis in cancer patients, but analysis of circulating erythroid precursors or liquid biopsy methods could be useful to detect induction of extramedullary erythropoiesis by these therapeutics. We are currently investigating the ability of CD47 antibodies to directly induce erythropoiesis using a human in vitro model.

> ***Reviewer #2 (Public Review):***
>
> *Summary:*
>
> *The authors used existing mouse models to compare the effects of ablating the CD47 receptor and its signaling ligand Thrombospondin. The CD47-KO model used in this study was generated by Kim et al, 2018, where hemolytic anemia and splenomegaly was reported. This study analyzes the cell composition of the spleens from CD47-KO and Thsp-KO, focusing on early hematopoietic and erythroid populations. The data broadly shows that splenomegaly in the CD47-KO is largely due to an increase in committed erythroid progenitors as seen by Flow Cytometry and single-cell sequencing, whereas the Thsp-KO shows a slight depletion of committed erythroid progenitors but is otherwise similar to WT in splenic cell composition.*

Strengths:

The techniques used are appropriate for the study and the data support the main conclusions of the study. This study provides novel insights into a putative role of Thsp-CD47 signaling in triggering definitive erythropoiesis in the mouse spleen in response to anemic stress and constitutes a good resource for researchers seeking to understand extramedullary erythropoiesis.

Weaknesses:

The Flow cytometry data alone supports the authors' main conclusion and single-cell sequencing confirms them but does not add further information, other than those already observed in the Flow data. The single-cell sequencing analysis and presentation could be improved by using alternate clustering methods as well as separating the data by genotype and displaying them in order for readers to fully grasp the nuanced differences in marker expression between the genotypes. Further, it is not clear from the authors' description of their results whether the increased splenic erythropoiesis is a direct consequence of CD47-KO or a response to the anemic stress in this mouse model. The enrichment of cKit+ Ter119+ Sca1- cells in CD47-KO indicates that these are likely stress erythroid progenitors. Another CD47-KO mouse model (Lindberg et al 1996) has no reported erythroid defects and was also not examined in this study.

(1) The reviewer asked, “whether the increased splenic erythropoiesis is a direct consequence of CD47-KO or a response to the anemic stress in this mouse model.” Our data supports both a direct role for CD47 and an indirect role resulting from the response to anemic stress. We cited our previous publications describing increased Sox2+ stem cells in spleens of *Cd47* and *Thbs1* knockout mice, but we neglected to emphasize another study where we found that bone marrow from *cd47−/−* mice subjected to the stress of ionizing radiation exhibited more colony forming units for erythroid (CFU-E) and burst-forming unit-erythroid (BFU-E) progenitors compared to bone marrow from irradiated wildtype mice (Maxhimer *Sci Transl Med* 2009). Taken together, our published data demonstrates that loss of CD47 results in an intrinsic protection of hematopoietic stem cells from genotoxic stress. This function of CD47 is thrombospondin-1-dependent and is consistent with the up-regulation of early erythroid precursors in the spleens of both knockout mice but cannot explain why the *Thbs1−/−* mice have fewer committed erythroid precursors than wildtype. We cited studies that documented increased red cell turnover in *cd47−/−* mice but less red cell turnover in *Thbs1−/−* mice compared to wildtype mice. Increased red cell clearance in *cd47−/−* mice is mediated by loss of the “don’t eat me” function of CD47 on red cells. In wildtype mice, clearance is augmented by thrombospondin-1 binding to the clustered CD47 on aging red cells (Wang, *Aging Cell* 2020). Thus, anemic stress in the mouse strains studied here decreases in the order *cd47−/−* > WT > *Thbs−/−*. This is consistent with the increased committed erythroid progenitors reported here in *cd47−/−* spleens and decreased committed progenitors in the *Thbs1−/−* spleens.

(2) Based on the reviewer’s question regarding alternative mechanisms and the publication of Yang et al 2022 identifying a role for CD47 in stress erythropoiesis though transfer of mitochondria to erythroblasts, we asked whether cd47-/- erythroid precursors would show decreased mRNA expression for mitochondrial chromosome genes (new Figure 4−figure supplement 3C). Some of these mRNAs were more abundant in cd47-/- and thbs1-/- erythroid cells, which is the opposite of what we expected based on Yang 2022 but consistent with our previous publications identifying thrombospondin-1 and CD47 as negative regulators of mitochondrial homeostasis in muscle cells and T cells.

(3) The *cd47−/−* mice used for the current study are the same strain as those reported by Lindberg et al in 1996, with additional backcrossing onto a C57BL/6 background.

> ***Recommendations For The Authors:***
>
> ***Reviewer #2 (Recommendations For The Authors):***
>
> *Suggestions for improved or additional experiments, data, or analyses.*
>
> *Significant efforts went into analyzing the type of erythroid progenitors by marker expression, but typical Flow cytometry strategies using Ter119 and CD44 combined with forward scatter can be used to stage the committed erythroid progenitors precisely.*

We appreciate this suggestion to extend the flow data. However, the upcoming retirement of the PI required closing our breeding colony, and the mice are no longer available.

> *How can the difference between the erythroid phenotypes of the Lindberg et al 1996 CD47-KO (exon2 Neo knock-in) and Kim et al 2018 CD47-ko (exon1 26bp indel) be explained?*

We are not convinced that the erythroid phenotypes of the Lindberg and Kim CD47-KO mice differ at the age used in our studies. Kim et al. focused on progressive hemolytic anemia and changes in T cells in spleen that emerge at 26 weeks age, whereas the mice used here were younger. The Lindberg and Kim mice have similar spleen enlargement at the age we used.

Another manuscript under review from our lab suggests that cis-regulation of an adjacent colinear gene could contribute to some phenotypes observed when perturbing the *Cd47* gene. The Lindberg mouse exhibits minimal perturbation of that adjacent gene, but we have no data regarding the Kim et al mouse. The reviewer's question brought to our attention that we neglected to state in the Methods that the mice used here are the Lindberg mice, not the Kim mice. This omission is now corrected.

> *The authors used Lindberg mouse for 2018 study on NK cells and observed splenomegaly. Did they check for extramedullary erythropoiesis there?*

Retrospective examination of the RNAseq data for the spleen cells enriched in NK precursors used in our 2018 publication (Nath, 2018) reveals significantly elevated expression for a majority of the extramedullary erythroid markers listed in Table 1, but they were generally less abundant than observed for the lineage-depleted spleen cells used in the present manuscript.

Author response table 1.

Extramedullary erythropoiesis Gene	CD47KO/WT_FC	CD47KO/WT_pval	DEG rank
Ermap	3.202941868	0.035938856	2087
Gypa	23.09289299	0.000169485	163
Gata1	2.809105664	0.044897197	2273
Slc4a1	4.352812248	0.005732723	1641
Klf1	30.09543812	0.000442139	76
Trim10	10.8936042	0.003179996	672
Sptb	4.443091877	0.00032532	1607
Rhag	25.90869436	8.45E-05	121

> *To clarify the stress erythropoiesis issue, it might be helpful to examine the sc-seq data for the expression of specific stress erythropoiesis markers in CD47-KO. Targets of BMP4 and Hedgehog signaling can also be examined. Further colony assays can help determine if stress BFU-Es are prevalent in the CD47-KO spleens and depleted in Thsp-KO*

As noted in Table 1, twelve of the genes we studied are established markers of stress-induced extramedullary erythropoiesis, and most of these were included in the scRNA seq data presented. Our previous publication demonstrated that bone marrow from cd47−/− mice subjected to the stress of ionizing radiation exhibited more colony forming units for erythroid (CFU-E) and burst-forming unit-erythroid (BFU-E) progenitors compared to bone marrow from irradiated wildtype mice (Maxhimer Sci Transl Med 2009). We have not performed colony formation assays using spleen.

To address the reviewer's question regarding BMP4 and hedgehog signaling we performed gene set enrichment analysis for known BMP4 and hedgehog signaling signatures. Using GSE26351_UNSTIM_VS_BMP_PATHWAY_STIM_HEMATOPOIETIC_PROGENITORS, cd47-/- cells in cluster 12 or their CD34+ orCD34- subsets did not show significant enrichment for BMP4 targets compared to WT. Thbs1-/- cells in clusters 12 and 14 showed marginally significant depletion of the BMP4 signature (p=0.04 and p=0.023, respectively). Using the KEGG_HEDGEHOG_SIGNALING_PATHWAY, we did not find any significant enrichment. However, only a few genes in this pathway were detectable in the scRNAseq data. These data suggest that the BMP4 signaling may be regulated by thrombospondin-1, but properly testing this hypothesis would require achieving greater sequencing depth combined with a cell isolation method that better enriches the early hematopoietic progenitors that are known to utilize the BMP4 pathway.

> *In the reclustering of erythroid progenitors in Figure 5, inclusion of Gata1 as a selection marker may help capture more of the early erythroid progenitors from the dataset and provide a more complete picture of the erythroid populations.*

We thank the reviewer for suggesting inclusion of Gata1. We repeated the reclustering including Gata1 and found the selected cell count increased from 876 cells to 1007 cells. However, most of the increase was not in the erythroid cluster, which increased from 413 cells to 419 cells. Most of the increase represented Gata1+ T cells (548 cells including Gata1 versus 463 cells without). The revised manuscript presents genotype-dependent differential gene expression based on including Gata1 selection, but none of the specific conclusions were changed from the initial submission. The new Table 4 and Figure 7−figure supplement 1 enabled us to compare differential expression of erythropoietic genes obtained using supervised and unsupervised clustering and show that both methods yield comparable results.

> *Just out of curiosity, was there an attempt to make a CD47 Thsp double KO? . Is it viable?*

Cd47 KO mice are somewhat difficult breeders, and several previous attempts to cross with other transgenics have produced viable homozygous offspring that could not be propagated.

> *Recommendations for improving the wring and presentation.*
>
> *Perhaps readers would find it more intriguing if the paper led with the single-cell sequencing showing enrichment of erythroid populations in CD47-KO, and later confirmed with Flow Cytometry (even if this was not necessarily the order in which the experiments were done).*

We considered this suggestion but believe that some of the flow cytometry data is needed to understand why we focused on CD34+ and CD34- subsets and proliferation markers when analyzing the scRNAseq data

> *The single-cell sequencing data in Figure 3 might benefit from UMAP clustering as well. In addition, it would greatly help readers if the data points were separated by genotype and displayed after clustering. A similar analysis has been done in this paper: doi:10.1038/s41556-022-00898-9 by clustering different conditions together but displaying them separately by condition.*

We initially explored tSNE and UMAP clustering and obtained similar results. We have added violin plots separated by genotype in Figure 4-figure supplement 2. We also included improved clusters separated by genotype in the revised Figure 3 panels C and D and for the reclustering in Figure 6D. UMAP plots provided better presentation for the reclustering (revised Figure 7). All data have been updated to the latest pipeline as noted in the Methods.

> *Minor corrections to the text and figures.*
>
> *Figure 4: Labels and plot legends are illegible in general, please relabel manually and if possible, redo plots with bigger font size and legends (relatively easy using ggplot2)*

All figure panels were relabeled using larger fonts

> *Figure 5D: Individual plots are stacked randomly atop each other and in many cases, gene names are not visible. Please restack the layers and ensure that the gene names are visible*

Panel D was made a separate figure with enlarged labels (now Figure 7).

> *Supp Fig 2: Layout can be organized a little better. Consider splitting into two figures for better organization*

The figure was split as recommended. Now Figure 1-figure supplement 2 and Figure 2-figure supplement

1.

> *Abstract Line 10: "...mRNA expression of Kit, Ermap, and Tfrc, Induction of committed erythroid precursors is...". Replace comma after "Tfrc" with period*

Done.

> *Discussion Page 9 Line 8: "...WT spleens, s. mRNAs for some markers of committed erythroid cells including Nr3c1 mRNA...". Remove ", s" after spleens.*

Done.

https://doi.org/10.7554/eLife.92679.2.sa3